N72-33765

18864-6004-RO-00

1 September 1972

FINAL REPORT OF THE OPGT/MJS PLASMA WAVE SCIENCE TEAM

Prepared by

F. L. Scarf, Team Leader

for

National Aeronautical and Space Administration
Washington, D.C. 20546

Contract NASW 2228

Space Sciences Department

TRW Systems Group
One Space Park
Redondo Beach, California 90278

1. TEAM ORGANIZATION AND MEMBERSHIP

The Plasma Wave Team Leader is Dr. F. L. Scarf of TRW Systems, and the official team members are Dr. D. A. Gurnett (University of Iowa), Dr. R. A. Helliwell (Stanford University), Dr. R. E. Holzer (UCLA), Dr. P. J. Kellogg (University of Minnesota), Dr. E. J. Smith (JPL), and Dr. E. Ungstrup (Danish Space Research Institute). Mr. A. M. A. Frandsen of JPL serves as Team Member and Experiment Representative.

In addition, the Plasma Wave Team solicited the continuing support and assistance of several other outstanding scientists, and we have designated these participants as Team Associates; the Associates are Dr. N. M. Brice (Cornell University), Dr. D. Cartwright (University of Minnesota), Dr. R. W. Fredricks (TRW), Dr. H. B. Liemohn (Boeing), Dr. C. F. Kennel (UCLA), and Dr. R. Thorne (UCLA).

2. GENERAL TEAM ACTIVITIES FEBRUARY 1972-AUGUST 31, 1972
(See the mid-year report for a summary of the earlier work)

During this period Dr. Scarf attended all SSG Meetings except the last one, where Dr. E. J. Smith represented the Plasma Wave Team. There were a number of Team Meetings and several additional conferences at JPL concerning EMI and other potential spacecraft problems.

The major development during this interval involved the decision not to go ahead with the Grand Tour. The change to the Mariner Jupiter/Saturn Mission required some redirection of the Headquarters-funded supporting studies. In particular, for the MJS 77 Jupiter flybys at L = 5.8 and L = 7.2, the

radiation hazard was no longer considered to be severe, and we terminated the JPL studies of radiation tolerance. Instead, the JPL Team Members focused attention on EMI problems and on the problems that developed in trying to fit a shielded magnetic search coil on the Mariner Astromast.

Dr. Scarf also redirected his efforts to study characteristics of the Saturn and Jupiter flybys, instead of considering all outer planets.

The general Stanford University study proceeded without change.

3. RESULTS

Our results are described in detail in a series of Appendices. Here we briefly summarize the contents of the individual sections.

1. A detailed study of the Plasma Environment and Magnetosphere of Saturn was carried out. The report is contained in Appendix 1. This paper was submitted to Cosmic Electrodynamics and is now in press.

2. Dr. Scarf analyzed the possible electrical hazards associated with differential spacecraft charging during the MJS flyby of Jupiter. A memo was transmitted to the Project, and a copy is contained in Appendix 2.

3. Dr. Scarf, Dr. Smith, and Mr. Frandsen conferred with the MJS Project on potential EMI problems and helped prepare specifications for the AFO package. Some memos on this topic are contained in Appendix 3.

4. Dr. Scarf prepared a handout for the final SSG Meeting, and Dr. Smith circulated this Summary of the Plasma Team effort to Headquarters personnel. A copy is contained in Appendix 4.

5. The Stanford Study directed by Dr. Helliwell was completed, and a Final Report is attached as Appendix 5.

18864-6004-RO-00

APPENDIX 1

to

FINAL REPORT OF THE OPGT/MJS PLASMA WAVE SCIENCE TEAM

18864-6003-RO-00

SOME COMMENTS ON THE MAGNETOSPHERE AND PLASMA ENVIRONMENT OF SATURN

by

Frederick L. Scarf
Space Sciences Department

20 April 1972

•Space Sciences Department
TRW Systems Group
One Space Park
Redondo Beach, California 90278

SOME COMMENTS ON THE MAGNETOSPHERE AND PLASMA ENVIRONMENT OF SATURN

ABSTRACT

Some properties of a model magnetosphere for Saturn are studied in order to determine the bounds that can be set on the surface field strength and the trapped particle population. The primary observational constraint is that non-thermal radiation similar to the Jovian radio emissions must be undetectable from Earth. It is argued that for a Saturn surface field of approximately one gauss, those particles that are energized as they diffuse in from the magnetopause with conservation of magnetic moment will produce synchrotron radiation levels that are undetectable at a range of 9.5 AU. The plasma instabilities that heat the oncoming wind particles at the bow shock and others that can limit the stably-trapped flux levels are also discussed briefly.

SOME COMMENTS ON THE MAGNETOSPHERE AND PLASMA ENVIRONMENT OF SATURN

1. INTRODUCTION

There is no direct evidence that the solar wind flows out to 9.5 AU in an ordered manner, but almost all theories of the heliosphere termination indicate that Saturn should be immersed in the wind (Axford, 1972). We also have no direct evidence that the magnetic moment of Saturn is finite, but the great physical similarities between Saturn and Jupiter suggest that it is very dangerous to assume that Saturn is unmagnetized. Therefore, we make the plausible assumptions that Saturn is magnetized and exposed to the solar wind, and we can then proceed toward construction of a general model for the planetary magnetosphere and trapped radiation belts. The single observational constraint, that Saturn should not produce non-thermal radio emission detectable on earth (Gulkis et al., 1969) appears easy to satisfy if we use the same type of reasoning that apparently works for Jupiter.

This note contains an outline of these concepts. In Section 2, the properties of the solar wind at 9.5 AU are considered. Section 3 contains an initial evaluation of the magnetospheric configuration, trapped radiation belts, and synchrotron emission for a one-gauss Saturn surface field. The role of plasma waves in controlling the wind-magnetosphere interaction and the trapped particle population of Saturn is discussed in Section 4. In the final section we summarize our considerations, and we argue that Saturn can indeed possess a significant magnetosphere with a sizeable trapped particle population. Thus, the non-detection of radio emission from Saturn must not be interpreted as evidence that Saturn has no magnetosphere.

2. THE SOLAR WIND AT 9.5 AU

No matter what general type of interaction occurs between a planetary object and the solar wind, the shock or interface actually forms within the interplanetary plasma. If the object is big enough, as Saturn certainly is, then a bow shock will develop, even for $B_s = 0$; in order to assess what this shock will look like, we have to know the ambient interplanetary characteristics.

It is actually a straightforward matter to extrapolate some solar wind parameters over the 1 AU to 9.5 AU range. We assume V(wind) = const (no heliosphere termination or neutral hydrogen "friction"), and this gives $N(r) \sim r^{-2}$. The same reasoning tells us that $B_r \sim r^{-1}$, $B_\theta \sim r^{-2}$ (the Parker model), and we readily find the numbers that are contained in Table 1, but some further comments are required to explain the significance of the last two entries.

Near Earth, the interplanetary right-hand polarized ($n^2 = R$) electron whistler mode wave appears to play a significant role in providing a dc magnetic field jump at the bow shock. For $f \simeq f_c^-/2$, this wave has a phase speed $\simeq cf_c^-/2\, f_p^- \simeq 900$ km/sec, and this is greater than the nominal 400 km/sec wind speed. As f increases past $f_c^-/2$ and toward f_c^-, the phase speed drops and for some intermediate f_o ($f_c^-/2 < f_o < f_c^-$), $(\omega/k) = V(\text{wind})$. In this case, the Doppler-shifted frequency $\omega' = \omega_o - \underset{\sim}{k}\cdot\underset{\sim}{V} = 0$, and a dc magnetic pulse stands in the wind to form a thin shock with $\lambda_o \simeq c/2\pi f_p^- \simeq 2$ kilometers. Table 1 shows that a similar situation can develop at Saturn, since $(\omega/k)_{MAX}$ at 9.5 AU $\simeq$ 770 km/sec is still greater than the wind speed. The main difference is that

Table 1. Solar Wind Parameters; Earth versus Saturn

Quantity	1 AU Nominal	9.5 AU Nominal
Velocity	400 km/sec	400 km/sec
Density	$5/cm^3$	$0.053/cm^3$
B_r	3.54γ	0.0393γ
B_θ	3.54γ	0.37γ
B	5γ	0.375γ
X	45°	89°
f_c^-	140 Hz	10.5 Hz
f_p^-	22 kHz	2.05 kHz
$\left(\frac{\omega}{k}\right)_{MAX}$ for $n^2 = R$	900 km/sec	770 km/sec
$\mu = \frac{\kappa T_\perp}{B}$	$\simeq$ 15 MeV/gauss	$\simeq$ 200 MeV/gauss

this type of bow shock would be somewhat thicker with $c/2\pi f_p^- \simeq 20$ km.

The final entry in Table 1 is related to the solar wind protons. The individual particles have the same total streaming energy ($\simeq$ 500 eV to 1 keV) at Earth or Saturn, and in both cases the post-shock protons with comparable energies can migrate into the planetary plasma environment to produce or contribute to the trapped proton belt. The Brice-Thorne-Coroniti-Kennel model

of the Jupiter proton belts (Brice, 1972; Thorne and Coroniti, 1972; Kennel, 1972) is based on diffusion with conservation of $\mu = mv_\perp^2/B$. Here we note that μ at Saturn is huge in comparison with the 1 AU value.

The thermal state of the solar wind at Saturn is much more uncertain. At 1 AU, we already have $T_- \neq T_+$, $(T_\parallel)_- \neq (T_\perp)_-$, $(T_\parallel/T_\perp)_- \neq (T_\parallel/T_\perp)_+$, where $\pm$ refer to electrons and protons, and the parallel-perpendicular subscripts refer to directions for thermal fluctuation speeds with respect to the magnetic field orientation. We don't really know how to account for the 1 AU temperatures, and any extrapolation is highly speculative. However, a number of simple physical models can be used. For instance, we can neglect the anisotropies (i.e., assume $K_\pm = (T_\parallel/T_\perp)_\pm \simeq 1$) and neglect the electron-proton temperature difference. Then a one-fluid (singly) adiabatic model gives $P = N\kappa T \sim N^\gamma$, or $T \sim r^{-2(\gamma-1)}$. For $\gamma = 3/2$, $T(r) \sim r^{-1}$. A two-fluid generalization of this is obvious, and a more sophisticated two-fluid "double adiabatic" model has $\kappa T_-/B$ = constant, $\kappa T_\parallel B^2/N^2$ = constant, for electrons and protons separately (see, for instance, Scarf, 1969). The results of these numerical explorations are gathered in Table 2, and several points are worth noting.

a) In all cases, $A_- = (2\kappa T_-/m)^{1/2}$ is quite low near Saturn, in comparison to the solar wind flow speed. For fast streams we could see $V(\text{wind}) \simeq A_-$. This is very significant because high frequency electrostatic plasma waves with $f = f_p^-$ have phase speeds near A_-. Thus, $\omega' = \omega - \underline{k}\cdot\underline{V}$ can be near zero in the planet frame, and a dc electric field jump can provide a new type of bow shock.

Table 2

Quantity	1 AU	9.5 AU	
$\langle T \rangle$	10^5°K	1.05×10^4°K	One-fluid singly adiabatic $\gamma = 3/2$
A_+	41 km/sec	13.3 km/sec	
A_-	1750 km/sec	570 km/sec	
$\langle T_+ \rangle$	5×10^4°K	5.2×10^3°K	Two-fluid singly adiabatic $\gamma = 3/2$
A_+	29 km/sec	9.5 km/sec	
$\langle T_- \rangle$	1.5×10^5°K	1.6×10^4°K	
A_-	2140 km/sec	690 km/sec	
$(T_+)_\parallel$	7.5×10^4°K	1.5×10^3°K	Two-fluid doubly adiabatic
$(T_+)_\perp$	3×10^4°K	2.24×10^3°K	
K_+	2.5	0.67	
A_+	29 km/sec	5.8 km/sec	
$(T_-)_\parallel$	1.6×10^5°K	3.45×10^4°k	
$(T_-)_\perp$	1.4×10^5°K	1.05×10^4°K	
K_-	1.14	0.314	
A_-	2140 km/sec	550 km/sec	

b) Near Earth $K_+ > 1$, $K_- \gtrsim 1$, and the solar wind is a plasma that is unstable with respect to growth of magnetosonic waves (the Firehose) and low frequency ($f \simeq f_c^+$) electron whistler mode waves (Kennel and Scarf, 1968). With the double adiabatic model, $K_+ < 1$ and $K_- < 1$ at $r = 9.5$ AU. In this case the solar wind is again unstable, but completely different plasma waves grow spontaneously. For $K_\pm < 1$, we should expect growth of ion and electron cyclotron waves ($n^2 = L$, $f \simeq f_c^+$, and $n^2 = R$, $f \simeq f_c^-$), and the wind at 10 AU should therefore be fundamentally different from that near earth (see also, Scarf, 1969).

3. THE MAGNETOSPHERE OF SATURN

Let us assume that Saturn has a centered dipole with moment $M = 2.16 \times 10^{29}$ cgs units and equatorial surface magnetic field equal to one gauss. This assumption is convenient and plausible because:

a) The f_c^- value at the surface is 2.8 MHz. If Saturn does have decametric-type radio emission, it would be invisible from Earth in this frequency range.

b) This value for $B_s(r_s)$ is about equal to one obtained with the assumption that the magnetic moment is proportional to the angular momentum. While a magnetic "Bode's Law" may be open to severe questioning for general applicability, it seems reasonable when we are merely comparing Saturn to Jupiter.

c) Brice and Ioannidis (1970, 1971) have carried out many calculations of magnetospheric shape, corotation effects, etc. for a one-gauss surface field plus a 10-hour spin period, and it is convenient to be able to draw on these reports.

With this assumption we can locate the subsolar magnetopause R-value using $(Nm_+V^2)_{wind} = R_s{}^6B_s{}^2(R=R_s)/8\pi R^6$. Using the parameters of Table 1 we then find R(mpause) $\simeq$ 39 R_s $\simeq$ 2.4 million kilometers. Thus, Saturn's magnetosphere can be intermediate between that of Earth (R $\simeq$ 10 R_e) and that of Jupiter (R $\simeq$ 53 R_J). The crucial question concerns the trapped population of Saturn's belts. What fluxes will be present? What will the particle energy distributions be? Why are non-thermal radio emissions undetectable?

Let us first consider the protons and their energies. As in the case of Jupiter (Brice, 1972, and the other Workshop papers), we assume that some fraction of the solar wind or magnetosheath population diffuses across a porous magnetopause conserving μ. If the particles then diffuse down to L = 2 (the known outer limit of the A-ring), still conserving μ, then $E_{(L=2)} \simeq E_{(sheath)}\,[B_{(L=2)}/B_{(sheath)}]$. At Saturn, $B_{(sheath)}$ is roughly one-half of the value at Jupiter (i.e., $B_{(interplanetary)}$ at 9.5 AU is about half the value at 5.2 AU), but we have assumed $B_{(surface)}$ at Saturn is one-twelfth of the value at Jupiter. This means E^+ (Saturn, L=2) $\simeq$ E^+ (Jupiter, L=2)/6. The upper limit Jupiter models of Brice (1972), Thorne and Coroniti (1972), and Kennel (1972) give a characteristic proton energy of 100 MeV at L = 2, and therefore at Saturn $E^+(L=2) \simeq E^+(maximum)$ might be near 15 MeV.

We can use precisely this idea to scale the electrons for Saturn. The cited upper limit model, and interpretations of Jovian radio emissions, give E^-(L=2, Jupiter) $\simeq$ 20 MeV, so that at Saturn we would not expect $E^-(L=2) = E^-(max)$ to be much greater than 3 MeV.

In fact, the origin of the high electron energy is rather obscure at Jupiter, and this number might well be an overestimate for Saturn, even if $B_s(L=1) = 1$ gauss. The point is that the solar wind electrons originally have very low values of $\mu = mV_\perp^2/B$. At Jupiter the incident electrons have $T_- \simeq 8 \times 10^3$°K, or $\mu = \kappa T^-/B \simeq 0.1$ MeV/gauss. A theory of the <u>electron</u> belts of Jupiter similar to the diffusion theory of the proton belts seems to require that the electrons become greatly energized at the shock so that μ^- jumps to perhaps 10 MeV/gauss in the Jovian magnetosheath.

However, at Saturn the electrons in the wind still have only about 0.1 MeV/gauss (T and B go as r^{-1}), and as we have seen in Section 2, the bow shock at Saturn may be vastly different from the one at Jupiter. It would seem prudent to take at least E^- fixed as proportional to $B_{surface} \times \mu^-(wind)$, and this gives $E^-(L=2;\ Saturn) \simeq E^-(L=2;\ Jupiter)/12 \simeq 1.7$ MeV.

This type of analysis can certainly be quite wrong in detail, but it does suggest a very plausible explanation for the non-detection of synchrotron radiation from Saturn. The energy radiated is

$$\left(\frac{dW}{dt}\right)_{synch} \simeq 4 \times 10^{-9}\, B^2 \sin^2\alpha\, E \left(1 + \frac{E}{2E_o}\right) \qquad (1)$$

where $E_o \simeq 0.5$ MeV. If $E(L) \sim B(L)$ by diffusion with conservation of μ, then $(dW/dt) \sim B_{max}^4$ $(E \gg E_o)$, or B_{max}^3 $(E \simeq 2E_o)$. A reduction in B from 12 gauss (Jupiter, L=1) to one-eighth of a gauss (Saturn at L = 2, or the outer edge of A-ring) therefore gives an intensity reduction that can exceed 10^8. Moreover, if the electron energies are as low as (1-3) MeV, then the beaming effect will

be greatly reduced. Finally, Saturn is observed at twice the distance of Jupiter, and this also lowers the flux received at Earth. It does seem from these considerations that we have no real reason to assume that Saturn is unmagnetized. It is more likely that the planet resembles Jupiter, with a weaker magnetic field that simply contains trapped particles of lower energy.

4. THE ROLE OF PLASMA WAVES

Wave-particle interactions must play a crucial role in governing the dynamics of the Saturn plasma environment, just as they do near Earth and at Jupiter. We can list a few distinct effects as follows:

a) Wave-particle interactions directly determine the energy transfer processes at the bow shock of Saturn. The wind is extremely dilute and cool here, and plasma instabilities provide the only mechanism for conversion of directed proton energy into thermal energy for magnetosheath electrons and protons. Since the magnetosheath particles are the ones that are incident on the magnetosphere and since they are also the basis for the ultimate energetic particle population, it is clear that the bow shock wave-particle interactions do play a fundamental role in the dynamics of the magnetosphere.

b) The incoming sheath particles become energized and anisotropic [$\kappa T_{\perp}^{\pm}(L) = \mu^{\pm} B(L)$] as they diffuse across L-shells, and this diffusion requires fluctuating E or B fields. High frequency waves allow fast (Bohm) diffusion (i.e., one gyradius per gyroperiod), but ULF fluctuations allow this to proceed much more slowly. The actual state is a balance of local effects; the

distribution depends on the wave spectrum via the cross-L diffusion coefficient, and it is also dependent on the pitch-angle diffusion coefficient (below). Thus, the total flux of trapped particles also directly depends on the local wave characteristics.

c) The loss-cone anisotropy ($T_\perp > T_\parallel$) must trigger ion and electron cyclotron turbulence that causes pitch angle diffusion and particle precipitation. This mechanism, which operates in the magnetosphere of the Earth [see Kennel and Petschek (1966) and Cornwall et al. (1970)], limits the flux of particles that can be stably trapped, and this also determines the overall intensity of the radio emission. The particles that are in resonance with cyclotron waves have $A_\pm = (T_\perp/T_\parallel)_\pm \geq A_c = [\Omega_c^\pm/\omega - 1]^{-1}$, and

$$E_{RES}^{\pm} \geq \frac{B^2}{8\pi N} [A_c^2(1+A_c)]^{-1} . \qquad (2)$$

A quantitative evaluation of the stably-trapped limit for Saturn requires knowledge of N(L). As with Jupiter, we expect a Brice-type cold plasma distribution governed by photoemission from the ionosphere and dominated by corotation out to the boundary at $R \simeq 39\ R_S$. However, a rigorous calculation of N(L) for Saturn (with 25 percent of the Jovian photoflux and a different ionospheric scale height) is not yet available. Therefore as a first working estimate we simply take $N_S(L) \simeq 0.25\ N_J(L)$, where N_J is the Brice-Ioannidis density profile. This initial model (which assumes that the reduced photoflux yields a corresponding reduction in photoelectron density) allows us to calculate all characteristic wave frequencies in the hypothetical magnetosphere of Saturn, and we can then also discuss the stable trapping phenomenon for Saturn. At the end of this section we discuss some more realistic density characteristics for Saturn.

It is useful to contrast the situations at Jupiter and Saturn, and accordingly Figure 1 compares the wave frequency versus L-value plots for both planets. Here we use $B_J(L=1) = 10$ gauss $= 10\ B_S(L=1)$, $N_J(L)$ = the Brice-Ioannidis profile, and $N_S(L) = N_J(L)/4$. The two plots are similar with shifts toward lower frequencies at Saturn, and some additional specific features are worth mentioning. In particular, it can be seen that while the surface electron gyrofrequency at Jupiter is several tens of MegaHertz (well above the Earth's ionospheric window), the model being used here predicts a surface gyrofrequency at Saturn of 2.8 MHz, or well below the window. Thus, as already noted at the beginning of Section 3, decametric-type radio emission from Saturn would not be detected by Earth-based radio telescopes with this model. However, the highest frequency emission from Saturn is probably much less than $f_c^-(L=1)$ because of the rings. If it is assumed that particles cannot be trapped on L-shells that intersect the rings, then shells with $L \lesssim 2.3$ (the outer limit of the A-ring) are removed from consideration, and the maximum equatorial gyrofrequency for an L-shell having a stable population is $f_c^-(\max) \simeq 530$ kHz. If this argument is expanded to exclude emission from $L \lesssim 4$ (the possible outer limit of the D´ring) then the highest equatorial gyrofrequency on an L-shell containing particles is $f_c^-(L=4) \simeq 44$ kHz, but the critical frequency at the density peak (near $L \simeq 9$-10) is $f_p^- \simeq 45$ kHz, and so none of this wave energy would be radiated from the planet.

In the diffusion models discussed above, the magnetosheath particles migrate inward from the dayside boundary with approximate conservation of magnetic moment, $\mu = mV_\perp^2/2B$. Thus, $A = (T_\perp/T_\parallel)$ increases with decreasing L and wherever Equation (2) is satisfied, the cyclotron resonance instabilities

then produce spontaneous growth of ion and electron whistler mode waves that scatter the particles and limit the trapped flux. This instability is important where the flux is high enough and where $(B^2/8\pi N)$, the minimum resonant energy, is less than the characteristic energy, $E_{\perp}(L) = \mu(mV_{\perp}^2/2) = \mu B(L)$. Using the $\mu^{(\pm)}$-values discussed above, the region of instability can be found graphically, and Figure 2 shows how $E_{\perp}^{(\pm)}$ and $(B^2/8\pi N)$ vary with L for Jupiter and Saturn. The Jupiter plot is essentially the same as the one presented by Thorne and Coroniti (1972), but the Saturn graph utilizes a μ^+-value twice as large as the Jupiter one (to account for the 50 percent decrease in the interplanetary field at 9.5 AU), while the μ^--value is kept fixed at 10 MeV/gauss (as discussed above). It can be seen that with these specific magnetospheric models the resonant particle instabilities can readily limit the trapped electron fluxes beyond L(Jupiter) $\simeq$ 7.2 or L(Saturn) $\simeq$ 6.5.

However, the resonant-particle electromagnetic cyclotron instabilities are not the only ones that are important in the Earth's magnetosphere. Recently, it was found that intense electrostatic waves with $f \simeq 3f_c^-/2$ develop and that these emissions can provide strong diffusion and precipitation for electrons (Kennel et al., 1970; Young, 1971; Scarf et al., 1972; Holzer and Sato, 1972). This electrostatic instability appears to develop when (f_c^-/f_p^-) is of order unity (Oya, 1972), and Figure 1 shows that for the models under consideration this condition occurs on slightly different L-shells at Jupiter and Saturn. Specifically, for Jupiter (f_c^-/f_p^-) equals unity near L = 7.7 while for Saturn the equality occurs near L = 5.9. Of course, this result depends in detail on the precise B and N models adopted for the two planets, and the numerical prediction cannot be taken very seriously. However, the disparity in the locations of the $(f_c^-/f_p^-) = 1$

regions does suggest an additional possible distinction between the Jupiter and Saturn magnetospheres. As noted in Figure 2, if the $3f_c^-/2$-scattering region for Jupiter is centered around L = 7.7 (say from L = 6.7 to L = 8.7), then the $3f_c^-/2$ instability overlaps the electromagnetic loss-cone instability that already can provide strong diffusion. Thus, the second electrostatic instability has a relatively minor effect here. However, if the electrostatic instability at Saturn is operative from L ≃ 4.9 to L ≃ 6.9, for instance, then this additional wave-particle scattering process extends the unstable region by a significant amount. Thus, for the Saturn model used here, it is conceivable that completely stable trapping would only develop in the narrow region between the outer limit of the A- or D´ring, and L ≃ 5.

Since all of these results do depend in detail on the selected $N_s(L)$ profile, it is worth considering qualitatively how a more realistic density estimate would change the characteristic frequencies and the hypothetical magnetosphere stability. A correct generalization of the Jupiter model has corotating photoelectrons of ionospheric origin populating the magnetosphere beyond the boundary where gravitational attraction balances the centrifugal force. At Jupiter this boundary is at about 2.2 R_J in the equatorial plane (Brice and Ioannidis, 1970), but Saturn has a somewhat smaller mass, and so for Saturn the same boundary is near r ≃ 1.8 R_s. In both of the outer planet cases the plasma should be in diffusive equilibrium at these radii, and any photoelectrons that have enough energy should populate the corotation region beyond the boundaries. However, one important correction becomes apparent here: Since an electron in synchronous orbit around Saturn has only about 35 percent of the kinetic energy of a synchronous electron around Jupiter, a larger fraction of the ionospheric photoelectron distribution will escape the

gravitational barrier, and thus beyond 1.8 R_S the plasma density at Saturn should be considerably higher than the value indicated by scaling the photoflux (I am indebted to Dr. C. F. Kennel for suggesting this important point). Thus, use of $N_s(L) \simeq 0.25\ N_J(L)$ actually gives a lower density limit for the inner magnetosphere of Saturn; for low L-values ($B^2/8\pi N$), is expected to be lower than the quantity shown in Figure 2, so that the inner magnetosphere of Saturn is probably more unstable than suggested above.

Another correction is required at higher L-values because the $N_s(L)$ profile should be limited by finite β effects. However, in Figures 1,2, the density is reduced by a factor of four and B^2 is reduced by a factor of one-hundred, so that at high L-values, the Saturn β adopted here is much higher than the reasonable values used by Brice and Ioannidis (1970). Thus, at Saturn, a realistic density profile should probably peak at a somewhat lower L-value, and it should remain lower than the $0.25\ N_J(L)$ curve beyond say L = 7. However, this change does not seriously affect the stability with respect to whistler mode turbulence since there is already a large instability margin beyond the peak density region.

5. DISCUSSION

Ground-based observers have never clearly detected non-thermal radio emissions from Saturn at any frequencies above the Earth's 10 MHz ionospheric window (Newburn and Gulkis, 1971). This result is frequently taken to imply that Saturn has no trapped particle belts, and in some discussions the negative result is interpreted as evidence that Saturn has no magnetic field at all. In fact, these conclusions do not follow from the radiometric data, and the main purpose of the present discussion is to demonstrate that plausible models of the Saturn magnetosphere, based on analogy with recent Jupiter models, provide no detectable radio emissions at Earth.

The basic point is that the electrons trapped in the magnetosphere of Jupiter attain extremely high energies (many tens of MeV) and produce such intense synchrotron radiation only because the Jovian magnetic field strength is so high. If we consider an analog of Jupiter with a surface field of one (rather than 10 or 12) gauss, then a number of phenomena combine to produce a tremendous decrease in the radiated power levels and beaming effects. The characteristic electron energy at a given L-shell will be down by an order of magnitude, and the radiated power will be decreased by three or four orders of magnitude [see Equation (1)], even if all other factors are constant. For Saturn, there are additional potential loss mechanisms associated with the rings, and local electromagnetic and electrostatic plasma instabilities may independently act to limit the trapped flux levels. Finally, if the surface field is as low as one gauss, the analog of the Jovian decametric radiation would occur at low enough frequencies so that the Earth's ionosphere would screen out the signal.

We conclude that the radiometric observations from Saturn are entirely consistent with a Jupiter-type magnetosphere model having a surface field on the order of one gauss. This result should not be surprising since the Earth, with a substantial population of energetic particles trapped in a 0.3 gauss surface field, provides no detectable synchrotron radiation at all. This experimental point is quite significant, and it is certainly well known that synchrotron radiation from the Earth would not be intense enough to be detected by an observer on Saturn. However, the case is even stronger than this: Natural synchrotron radiation from the Earth's trapped particle belts has not even been clearly detected by radio experiments traversing the belts

in Earth orbit (R. G. Stone, private communication). In fact, the only unambiguous published accounts of synchrotron radiation from the Earth's belts are associated with the artificial injection of relativistic electrons into trapped orbits following the July 9, 1962 high-altitude nuclear explosion (Ochs et al., 1963; Dyce and Horowitz, 1963; Peterson and Hower, 1963).

Thus, it is prudent to approach the problem of exploring Saturn assuming that it does have a magnetic field and trapped particle population, with the radiometric observations being used to set a plausible limit of about one gauss for a surface field. There is presently no well-founded theory of planetary magnetism that can be used to provide a better estimate, but Saturn is somewhat smaller than Jupiter and the surface field reduction by an order of magnitude seems reasonable. For instance, Saturn's mass, angular momentum, and volume are about 30 percent, 22 percent, and 60 percent of the corresponding quantities for Jupiter (in the respective order), so that many semi-empirical models would predict a smaller planetary field. The use of a model one-gauss surface field is therefore suggested until direct flyby measurements provide more precise information.

ACKNOWLEDGMENTS

Several ideas discussed in this note were directly stimulated by the presentations of Drs. N. M. Brice, F. V. Coroniti, C. F. Kennel, and R. M. Thorne at the Jupiter Radiation Belt Workshop. I am also grateful to Dr. Kennel for some helpful comments about possible density distributions in the magnetosphere of Saturn, and I thank Dr. Thorne for permission to adapt one of his drawings for the upper part of Figure 2. This work was supported by the National Aeronautical and Space Administration under Contract NASW -2228.

REFERENCES

Axford, W. I.: 1972, in Proc. Asilomar Conf. on the Solar Wind, in press.

Brice, N. M. and Ioannidis, G. A.: 1970, Icarus 13, 173.

Brice, N. M.: 1972, in Proc. of the Jupiter Radiation Belt Workshop, Jet Propulsion Laboratory, in press.

Cornwall, J. M., Coroniti, F. V., and Thorne, R. M.: 1970, J. Geophys. Res. 75, 4699.

Dyce, R. B. and Horowitz, S.: 1963, J. Geophys. Res. 68, 713.

Gulkis, S., McDonough, T. R., and Craft, H.: 1969, Icarus 10, 421.

Holzer, T. E., and Sato, T.: 1972, submitted to J. Geophys. Res.

Ioannidis, G. A. and Brice. N. M.: 1971, Icarus 14, 360.

Kennel, C. F. and Petschek, H.: 1966, J. Geophys. Res. 71, 1.

Kennel, C. F. and Scarf, F. L.: 1968, J. Geophys. Res. 73, 6149.

Kennel, C. F., Scarf, F. L., Fredricks, R. W., McGehee, J. H., and Coroniti, F. V.: 1970, J. Geophys. Res. 75, 6136.

Kennel, C. F.: 1972, in Proc. of the Jupiter Radiation Belt Workshop, Jet Propulsion Laboratory, in press.

Newburn, Jr., R. L. and Gulkis, S.: 1971, Jet Propulsion Laboratory Technical Report 32-1529.

Ochs, G. R., Farley, Jr., D. T., Bowles, K. L., and Bandyopadhay, P.: 1963, J. Geophys. Res. 68, 701.

Oya, H.: 1972, submitted to J. Geophys. Res.

REFERENCES (Cont'd)

Peterson, A. M. and Hower, G. L.: 1963, J. Geophys. Res. 68, 723.

Scarf, F. L.: 1969, Planet. and Space Sci. 17, 595.

Scarf, F. L., Fredricks, R. W., Kennel, C. F., and Coroniti, F. V.: 1972, submitted to J. Geophys. Res.

Thorne, R. M. and Coroniti, F. V.: 1972, in Proc. of the Jupiter Radiation Belt Workshop, Jet Propulsion Laboratory, in press.

Young, T. S. T.: 1971, Ph.D. Thesis, Report LPP-1, Massachusetts Institute of Technology.

FIGURE CAPTIONS

Figure 1. Equatorial characteristic frequency profiles for the model magnetospheres of Saturn and Jupiter. It is assumed that the magnetic fields are centered dipoles, and that the densities are represented by Brice-Ioannidis functions. The positions of the planetary satellites and the Saturn rings are noted at the top. Here $f_c^{\pm}$ represent the electron and proton gyrofrequencies, the plasma frequencies are $f_p^{\pm}$, f_{UHR} is the upper hybrid frequency, and f_{LHR} is the lower hybrid frequency. It is likely that the actual density profile in the magnetosphere of Saturn is higher than 0.25 $N_J(L)$ within about L = 7, and lower than 0.25 $N_J(L)$ beyond (see discussion in text).

Figure 2. Comparison of model electron-proton energy profiles for Jupiter and Saturn with $B^2/8\pi N$, the minimum resonant energy that leads to strong pitch angle scattering via the cyclotron-resonant loss-cone instabilities. The $(3f_c^-/2)$ scattering regions occur where (f_c^-/f_p^-) is of order unity (see Figure 1). The models used here indicate that the trapped electron flux at Saturn has relatively low characteristic energy, and that there are potentially important loss mechanisms associated with the rings and with the $(3f_c^-/2)$ wave-particle interactions. A more realistic density profile for Saturn would probably enhance the whistler mode instability at lower L-values.

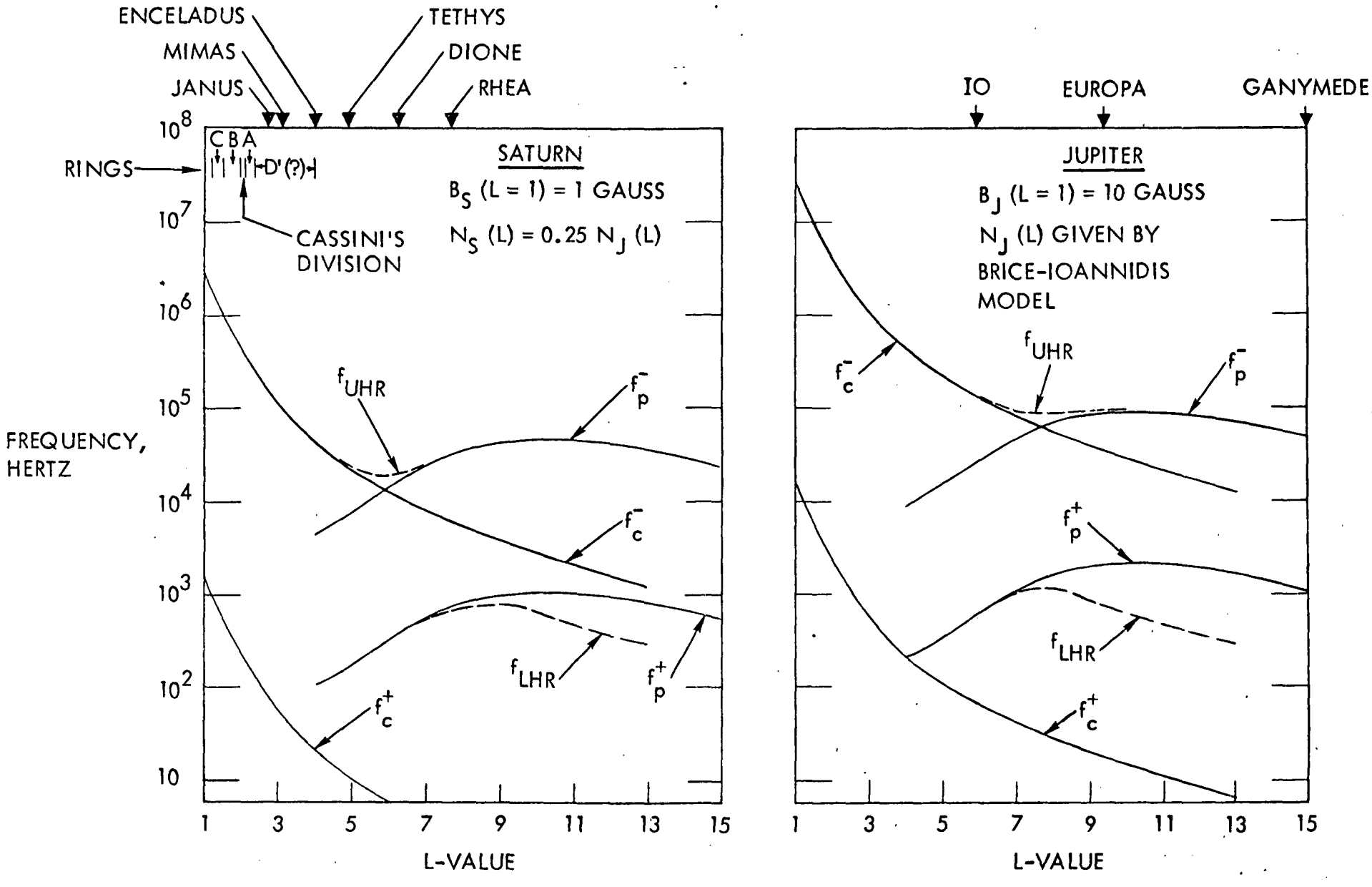
ENCELADUS
TETHYS
MIMAS
DIONE
JANUS
RHEA
RINGS
C B A
D' (?)
CASSINI'S DIVISION
SATURN
B_S (L = 1) = 1 GAUSS
N_S (L) = 0.25 N_J (L)
IO
EUROPA
GANYMEDE
JUPITER
B_J (L = 1) = 10 GAUSS
N_J (L) GIVEN BY BRICE-IOANNIDIS MODEL
FREQUENCY, HERTZ
10^8
10^7
10^6
10^5
10^4
10^3
10^2
10
f_{UHR}
f_p^-
f_c^-
f_{LHR}
f_p^+
f_c^+
1 3 5 7 9 11 13 15
L-VALUE

Figure 1

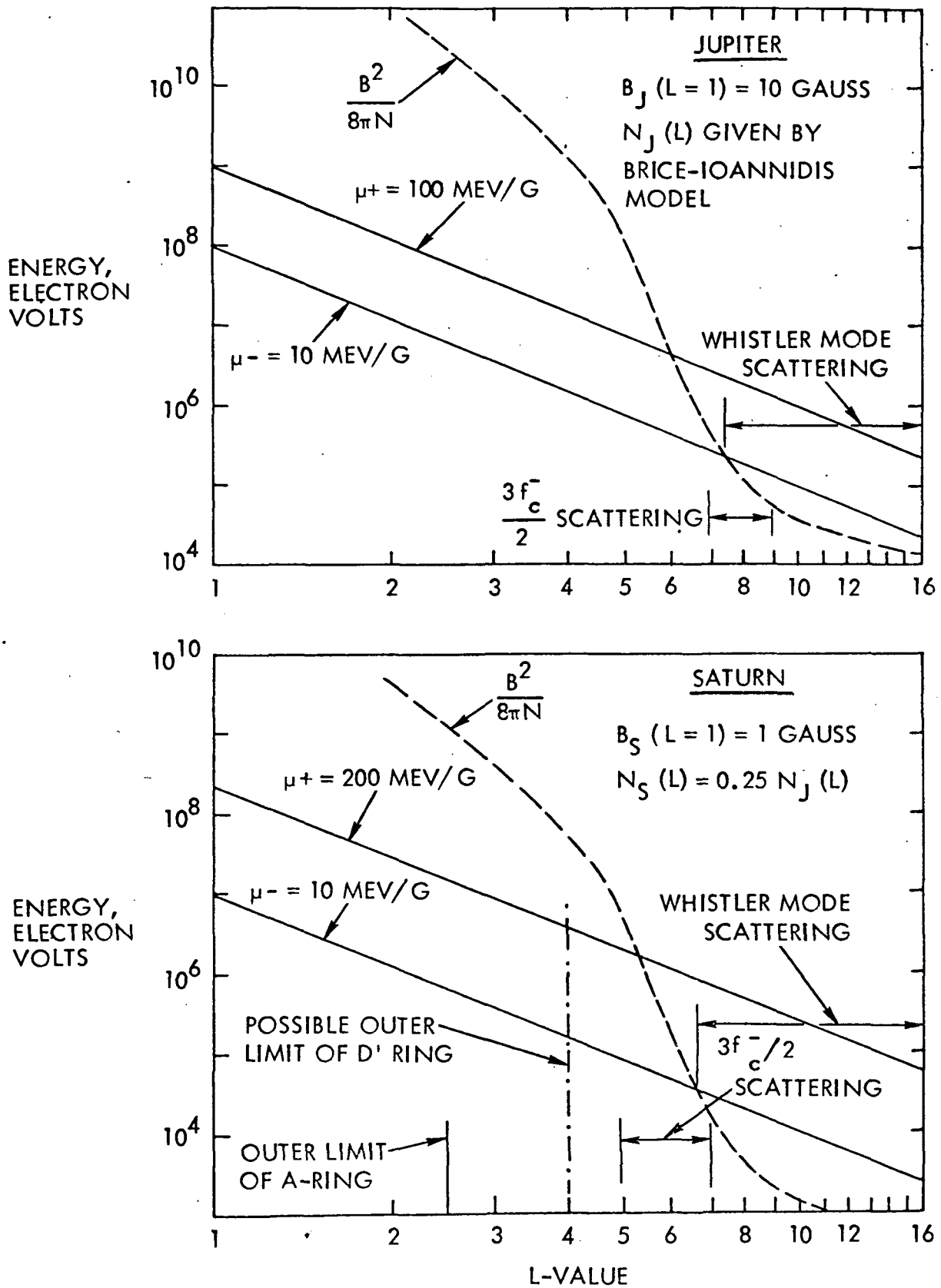
JUPITER
B_J (L = 1) = 10 GAUSS
N_J (L) GIVEN BY BRICE-IOANNIDIS MODEL
$\frac{B^2}{8\pi N}$
μ+ = 100 MEV/G
μ- = 10 MEV/G
WHISTLER MODE SCATTERING
$\frac{3f_c^-}{2}$ SCATTERING
ENERGY, ELECTRON VOLTS
10^{10}
10^8
10^6
10^4
1 2 3 4 5 6 8 10 12 16
SATURN
B_S (L = 1) = 1 GAUSS
N_S (L) = 0.25 N_J (L)
$\frac{B^2}{8\pi N}$
μ+ = 200 MEV/G
μ- = 10 MEV/G
WHISTLER MODE SCATTERING
POSSIBLE OUTER LIMIT OF D' RING
$3f_c^-/2$ SCATTERING
OUTER LIMIT OF A-RING
ENERGY, ELECTRON VOLTS
L-VALUE

Figure 2

18864-6004-RO-00

APPENDIX 2

to

FINAL REPORT OF THE OPGT/MJS PLASMA WAVE SCIENCE TEAM

8301-72-83
Bldg R-1, Rm 1070
2 May 1972

To: E. J. Smith

From: F. L. Scarf

Subject: Possible Spacecraft Charging Problems near Jupiter

1. Background

Recently, de Forest (JGR, February 1, 1972) showed that the 10-20 keV electrons encountered in earth orbit ($r \simeq 6.6$ Re) during substorm injection events cause overall potential shifts (relative to the plasma) on the order of (1-10) kV. Moreover, differential charging produces local E-fields ranging up to several hundred volts/meter. In fact, we can anticipate that if ATS-5 primarily had insulation (rather than an aluminum band) surrounding the spacecraft equator, then the local fields could have been as high as (1-10) kV/meter. In essence, the illuminated side would develop one potential (say -300 volts), while the dark side would charge to about 1 to 10 kV negative. There is also evidence that in earth orbit some other spacecraft with insulated outer surfaces have actually experienced local potential gradients greater than 1 or 2 kV/meter during multiple substorm injection events; these very large local fields develop when the initial substorms have removed the quiescent cold plasma, and the remaining plasma then has $\kappa T_e \sim$ 10-20 keV. If we ignore secondaries, and scattered particles, then the sunlit side of the spacecraft (or one of its subsystems) has

$$e\phi \simeq -\kappa T_e \ln \left[\frac{N_e \sqrt{\kappa T_e / m_e}}{j(\text{photo})} \right] \qquad (1)$$

and the dark side has

$$e\phi \simeq -\kappa T_e \ln \sqrt{\frac{T_e m_p}{T_p m_e}} \qquad (2)$$

Here $j(\text{photo}) \simeq 5 \times 10^9\ (\text{cm}^2\text{sec})^{-1}$, N_e is typically (1-10) cm^{-3}, $\kappa T_e \simeq$ 10-20 keV, and $T_p \gtrsim T_e$. Since κT_e is so large, even small differences between the logarithmic factors can provide very high local electric field strengths.

2. Relevance to Jupiter

The substorm electrons observed by ATS-5 are thought to achieve their high energies by convecting inward toward the earth with conservation of $\mu = mv_\perp^2/B$. Precisely the same process is involved at Jupiter, but B is much larger and hence the electron energies become much larger. The radiation workshop (and the analysis of Jupiter's radio emissions) gives $\kappa T_e \simeq 20$ MeV from L = 1 to L = 2! Clearly, if there is not a sufficiently dense cold plasma, then differential charging effects can give local E-fields at Jupiter three orders of magnitude larger than corresponding values seen in earth orbit.

The Brice model of the Jupiter cold plasma ($\kappa T \simeq$ 5-10 eV) distribution does predict a fairly high density in the spin-equatorial plane. The enclosed figures compare the fluxes of energetic protons and electrons (radiation workshop upper limit) with $[N(\kappa T/m)^{1/2}]_\pm$ given by the Brice model. On the proton chart we also show $j(\text{photo; Jupiter}) \simeq j(\text{photo, earth})/27 \simeq 2 \times 10^8\ (\text{cm}^2\text{sec})^{-1}$. There are also some predictions of the Brice-type models for locations away from the equator. The cold plasma density falls off as $N \sim \exp(-\Delta r/H)$, where $H \simeq 0.5\text{-}1.0\ R_J$, and Δr is the displacement along the field line from the equator. Note that at high latitudes (e.g., the planned 45° Pioneer G encounter) there are essentially no cold particles. Thus, κT_e in Equations (1),(2) will be given by the radiation workshop model (many MeV) for a high latitude trajectory.

Assuming that Brice is right, then even near the equator, large voltage pulses will develop in the plasma sheath. Within L $\simeq$ 2-4, j_e (many MeV) >> j_e (10 eV), and in Equations (1),(2), we would use $\kappa T_e \simeq E_o$ (the radiation workshop characteristic energy); thus, differential charging would give $\Delta\phi/\Delta\ell \simeq$ (several MV/(characteristic length).

Even beyond L ≃ (2-4), significant potential gradients can develop with this model. For instance, at L = 20, $j_e \simeq 10^9$, $j_+ = j_+(\text{photo}) \simeq 2 \times 10^8$, and $\kappa T_e \simeq 10$ eV. Thus, the sunlit side charges to $-e\phi \simeq 10$ eV ℓn 5, while the dark side charges to $-e\phi \simeq 10$ eV ℓn 43, and $\Delta\phi$(sun to shade) ≃ 20 volts. Any scanning device that produces a variable shadow can therefore also produce a fairly large amplitude voltage ripple in the sheath. Moreover, as the spacecraft enters sun-shadow, there has to be an overall voltage pulse of this magnitude.

3. Assessment of Potential Problems

If one believes the interpretation of the Jovian radio emissions and the predictions of the Brice model, then MeV differential charging will occur within L = 2-4 on the equator, and over a rapidly increasing spatial region at higher latitudes. Elsewhere, differential charging will give electric field pulses of about 20 volts/meter (or more, depending on the scale sizes in the spacecraft).

However, while we know that the energetic particle fluxes are really present, it should be remembered that the Brice model is only a theoretical prediction. The Faraday rotation data do suggest that N(L) should be smaller than predicted, and the MeV (or keV) charging problems could easily extend over a much broader region than indicated above. Therefore, differential spacecraft charging in the Jupiter magnetosphere has to be thought of as a real hazard.

4. Solutions

As de Forest noted (JGR, page 659, 1972), "Although much labor is spent in making spacecraft magnetically clean, much less effort seems to have gone into making spacecraft electrostatically clean". In order to avoid or minimize the potential hazards discussed above, one must construct MJS with a grounded electrostatic shield or Faraday cage around all subsystems. Thermal insulation can be put on the outside, but the electronics devices have to be protected from sheath-induced voltage transients.

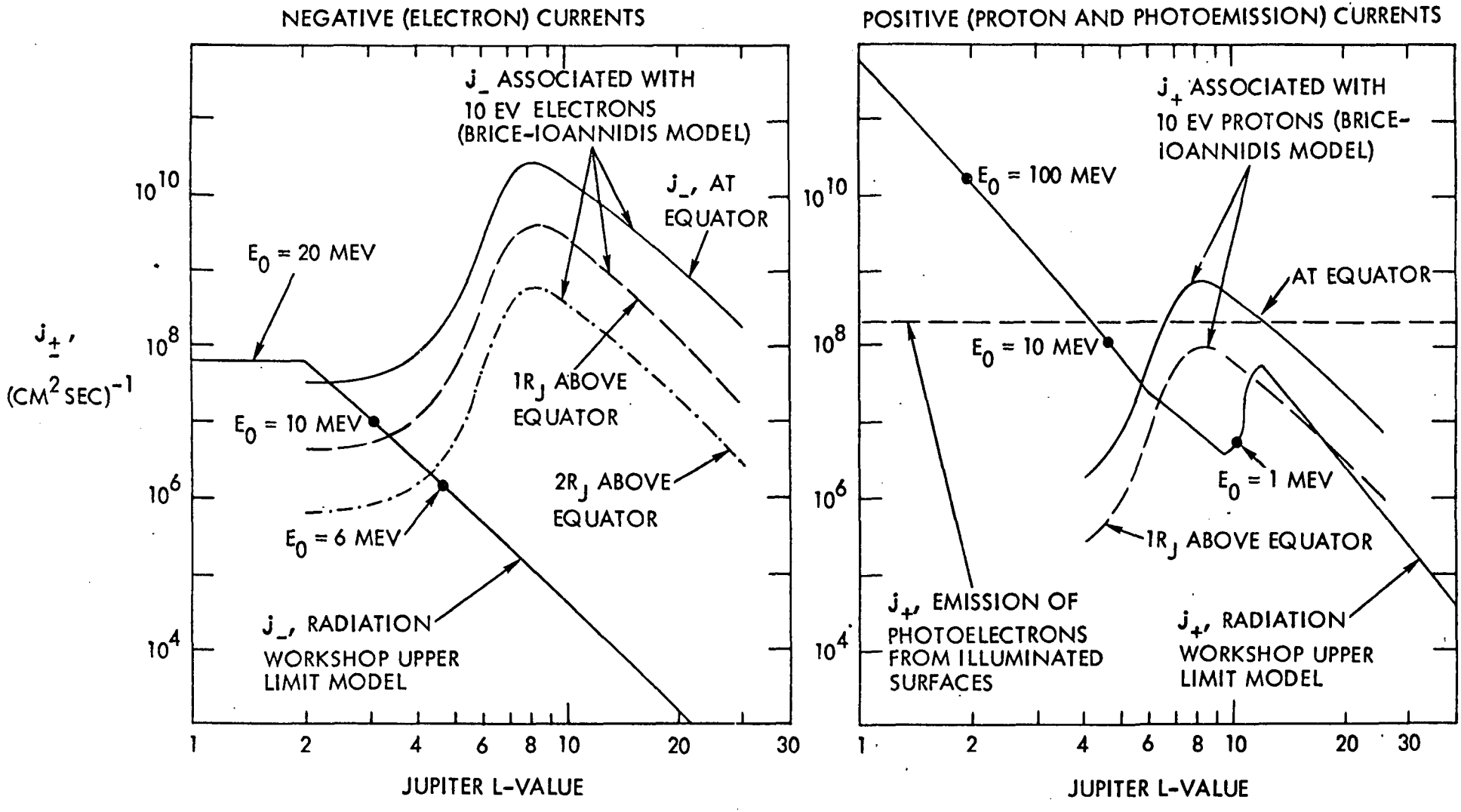
NEGATIVE (ELECTRON) CURRENTS
POSITIVE (PROTON AND PHOTOEMISSION) CURRENTS
j_ ASSOCIATED WITH 10 EV ELECTRONS (BRICE-IOANNIDIS MODEL)
j_, AT EQUATOR
E0 = 20 MEV
E0 = 10 MEV
E0 = 6 MEV
1RJ ABOVE EQUATOR
2RJ ABOVE EQUATOR
j_, RADIATION WORKSHOP UPPER LIMIT MODEL
j+ ASSOCIATED WITH 10 EV PROTONS (BRICE-IOANNIDIS MODEL)
E0 = 100 MEV
AT EQUATOR
E0 = 1 MEV
1RJ ABOVE EQUATOR
j+, EMISSION OF PHOTOELECTRONS FROM ILLUMINATED SURFACES
j+, RADIATION WORKSHOP UPPER LIMIT MODEL
j±, (CM2 SEC)-1
10^10
10^8
10^6
10^4
1
2
4
6
8
10
20
30
JUPITER L-VALUE
JUPITER L-VALUE

APPENDIX 3

to

FINAL REPORT OF THE OPGT/MJS PLASMA WAVE SCIENCE TEAM

8301-72-86
Bldg R-1, Rm 1070
5 May 1972

Dr. E. J. Smith
Space Sciences Division
Jet Propulsion Laboratory
4800 Oak Grove Drive
Pasadena, California 91109

Dear Ed:

Several people left the May 3 EMC Specification Meeting with very disquieting feelings about the suitability of using present Mariner or Viking spacecraft fabrication techniques without change for the MJS mission. For the past year we have talked about a payload that is about half particles, waves and fields, and this type of payload has been widely advertised to SAG, SSB, and others. Yet if MJS is really built with unshielded boxes and cables, and with minimum or non-existent EMC specifications on spacecraft subsystems, then modern particle, field and wave instruments will not work on the spacecraft. For instance, as discussed at the meeting, energetic particle experiments on Pioneer 9 (Webber) and on IMP-6 (McDonald) gave spurious readings in initial ground tests because of noise on the engineering lines. These problems were fixed up, and the instruments work perfectly in space. However, IMP and Pioneer, as well as OGO, Injun, Vela, all recent Air Force spacecraft, etc. are built to operate with a variety of magnetospheric instruments, and they all have grounded shields around <u>every</u> electronic subsystem, power cable, etc.

The argument presented at the meeting (that previous Mariners haven't had trouble) is really irrelevant. The last Mariner to carry particles and fields instruments was Mariner 5, and this used rather old experiment technology. We are now asking people to draw on recently developed instrument techniques. I assume that MJS is intended to carry out comparative Saturn-Jupiter investigations that are at least as sophisticated as the one now being carried out on Pioneer F,G. Yet all the Pioneer F,G electronics is within a shielded container, and all spacecraft subsystems and cabling are shielded. I doubt very much that any of the four Pioneer F,G energetic particle experiments could operate correctly within an open compartment, with 100 volt peak to peak square waves at 2.4 kHz, and no shielding of any spacecraft subsystems. Of course, many experimenters will propose on the basis of IMP H,I,J technology, and these very modern instruments will certainly not tolerate the noise environment presently contemplated.

I am using particle experiments as examples here because the basic problem is more or less independent of the payload specifics, but of course potential wave experiments can be strongly degraded if local noise is not controlled. I do not think that this control requires great expense -- instead we need a significant change in the philosophy of subsystem packaging, cabling, grounding, that has a minor cost implication. As an example, I recently reviewed some reports on a wave experiment that Forrest Mozer flew on OV-1-18. As you know, the OV-1 satellites are very inexpensive, piggyback spacecraft built to accomodate a variety of payloads with minimum integration expense and problems; therefore, using simple but modern techniques (shielding, grounding, etc.), interference is controlled, and in flight Mozer actually could not detect any spacecraft noise signals at all.

I hope that the MJS project will consider these points. We can certainly use Viking and Mariner devices and technology, but it can't cost very much to change the packaging and shielding techniques.

Sincerely yours,

Fred

Frederick L. Scarf
Leader, MJS Plasma Wave Team
TRW Systems Group

FLS:jg

cc: K. Anderson
M. J. Belton
J. Blamont
P. J. Coleman
T. Donahue
V. R. Eshelman
B. Farmer
A. Goetz
R. Soberman
R. Vogt
J. Warwick
J. Wolfe

P.S. These arguments concern the operation of MJS in cruise and near Saturn. At Jupiter you still have to cope with volt/meter RF fields, and low frequency emissions and sheath fields that may be very intense. Don't you think that better EMC is needed just to get past Jupiter safely?

JET PROPULSION LABORATORY

INTEROFFICE MEMORANDUM
2946-72-40/2949-72-41

15 May 1972

TO: R. L. Heacock

FROM: T. E. Gindorf/J. G. Bastow

SUBJECT: EMC Testing of Viking Hardware in Support of MJS'77

Some of the field and wave experimenters interested in MJS'77 opportunities have expressed concern about the EMC practices followed on Mariner spacecrafts. If a comparison is made with other NASA programs, it is readily apparent that the EMC testing effort is much smaller on JPL programs. In the past this effort has been adequate because the spacecraft have carried a minimum of sensitive wave and field experiments.

Two major problems are created by the Mariner style of open subassembly packaging. First, any circuitry or wiring not shielded from the interplanetary plasma results in a coupling of signals and noise on the circuit or wire directly into the Plasma Wave/Radio Astronomy E-field antennas. This condition can only be resolved by ensuring that the complete external surface of the spacecraft is a continuous electric shield and that all wires that penetrate outside this shield are also shielded.

The second problem is the coupling of extraneous signals and noise between subassemblies within the spacecraft bus either directly between unshielded subsystem circuits, or by means of unshielded or poorly shielded wires and cables. Such interference causes a more serious problem to sensitive analog experiments than it does to engineering subsystems or less sensitive experiments. In the latter cases immunity can be built into the subsystems in many cases and the level of allowable interference can be quite high if intended signals are also relatively high (on the order of volts), as is most often the case. This is the philosophical basis for Viking conducted noise generation and immunity requirements. With wave and field experiments, however; all interference is detrimental. Even though it cannot be completely eliminated, any interference reduction is beneficial. From a science point of view, significant reduction has been described as essential and has been achieved on other spacecraft, notably IMP-I.

Although the open style subassembly packaging has been employed by JPL for a considerable length of time, most non-JPL spacecraft subsystems (Pioneer, OGO, IMP, etc.) have been completely

contained in shielded enclosures. It is impossible to confidently estimate the interference generated by Mariner type subassemblies as virtually no measurements have been made of either the generated conducted or radiated interference as a function of frequency in the MIL Spec manner since 1963. Consequently, it is currently impossible to comprehend either what the real adverse effects would be on sensitive experiments or to what extent corrective EMC measures could economically be adapted on JPL spacecraft. It is safe to say that we have made little real progress with EMC since Ranger and actually are only scratching the surface in the Viking program. To some extent prior spacecraft have not required stringent control because of less sensitive experiments or spacecraft subsystems. As a point of reference, the EMC requirements on the JPL ORBITER are considerably less stringent than those being imposed on the MARTIN LANDER. It is unfortunate that progressive design and test improvement has not been made in EMC at JPL as has been done with other environmental disciplines.

It is strongly recommended that the MJS'77 project persuade the Viking Orbiter project to conduct (with assistance as requested), passive EMC measurements on inherited Viking prototype or type approval hardware at the earliest practical date. Such measurements could be integrated into the present more limited Viking subsystem test program with minimum impact or cost. Such information would serve as a basis for understanding necessary corrective measures on the MJS'77 and future programs and also provide experimenters with information essential to adpating their experiment to the spacecraft environment. This testing, involving about seven subsystems would probably require an additional day for those subsystems to be EMI tested in-house and two days at JPL for those to be tested for Viking at contractor facilities. Equipment and facilities required for these tests are available on Lab. Total added cost would be on the order of $20K. These tests would furnish early information on the adequacy of JPL/Mariner class spacecraft as compared to the Pioneer spacecraft in providing a suitable platform for field, particle and wave experiments and indicate the degree of improvement necessary in Viking hardware.

J. G. Bastow/T. E. Gindorf
Environmental Requirements Section

JGB/TEG:hem

cc: D. T. Frankos
A. M. Frandsen
D. S. Hess
R. F. Draper
W. S. Shipley
E. J. Smith
H. M. Schurmeier

CONFERENCE REPORT

JET PROPULSION LABORATORY

REPORT NO._____

SUBJECT Summary of an MJS Electromagnetic Compatibility Meeting

PROJECT MJS'77 CONTRACTOR _____ CONTRACT or

ACTION REQUIRED BY _____

TELECON Initiated by _____	Report Prepared by A.M.A. Frandsen
CONFERENCE at JPL, 183-427	Date Prepared 5/15/72
Date of Occurrence May 3, 1972	Revised 5/25/72

Participants		Distribution	
J. G. Bastow,	JPL	Participants, MJS Plasma Wave Team, MJS Radio Astronomy Team,	
T. N. Divine,	JPL	T. H. Bird,	JPL
R. F. Draper,	JPL	C. B. Farmer,	JPL
A. M. A. Frandsen,	JPL	W. G. Fawcett,	JPL
T. E. Gindorf,	JPL	H. L. Friedman,	JPL
D. P. Martin,	JPL	J. K. Haas,	JPL
R. Pelzer,	U. of Mich.	R. L. Heacock,	JPL
W. Pfeiffer,	U. of Iowa	M. A. Mitz,	NASA HQ
F. L. Scarf,	TRW	D. G. Rea,	JPL
E. J. Smith,	JPL	L. L. Simmons,	JPL
R. L. Stoller,	JPL	H. M. Schurmeier,	JPL
J. W. Warwick,	U. of Colo.	F. H. Wright,	JPL
R. Weber,	GSFC		

On May 3, 1972 members of the MJS Plasma Wave and Radio Astronomy teams met with members of the MJS'77 Project to: 1) Specify the levels of spacecraft generated electromagnetic interference (EMI) which they consider acceptable to their investigations and 2) Discuss the types of EMI which all spacecraft subsystems can expect to experience in the near Jupiter environment.

At the plasma wave loop antenna, the acceptable level of magnetic interference was stated as 0.01γ rms in any 10% bandwidth between 10 Hz and 200 KHz. By locating the loop antenna ~ 10 meters outboard on the Astromast boom, the plasma wave experiment's permissible interference level at 10 Hz can be made consistent with the 10 Hz requirement imposed by the magnetometer experiment.

With regard to the acceptable levels of electric field interference, the Plasma Wave team requested a specification which allows interfering E fields of no more than 10 μv rms/meter in any 10% bandwidth between 10Hz and 100 KHz. The Planetary Radio Astronomy team requested that E field interference levels not be allowed to exceed a flat spectral density corresponding to 1 μv rms/meter in a 10% band at 100 KHz.

From the discussion that followed, there appeared to be little chance of meeting either teams' electric field interference requirements with the packaging philosophy traditionally used on the Mariners. The problem is difficult for any spacecraft carrying monopoles mounted on the structure. It is difficult because the residual electric field interference that gets outside the spacecraft skin can be expected to couple directly into the monopoles through the surrounding plasma sheath, with very little attenuation. In principle, the problem should be less difficult to solve on an MJS spacecraft because one major source of interference coupling, namely the power converter and system noise fed back onto unshielded solar panel bus wires, will not be present on these missions. However, the electrostatically "open" construction of the Mariners more than offsets this advantage. A spacecraft construction method more compatible with having sensitive electric field experiments on the payload is the shielded-box-within-a-shielded-box approach used on Pioneer, OGO, Imp and others.

Fred Scarf pointed out that even if there were no wave experiments on the payload, the MJS project should consider changing to a shielded box construction for the following three reasons:

a) In the interest of spacecraft survival at Jupiter, all spacecraft subsystems must be protected from the volts per meter electric fields emanating from Jupiter's naturally occurring sources of decametric radio noise. (Bob Pelzer points out that this is not unlike requiring the spacecraft to operate within a screen room containing a strong RF transmitter).

b) The spacecraft subsystems must be protected from the effects of arcing caused by the large differential electrostatic charging phenomena likely to occur within Jupiter's plasmasphere.

c) A payload which has been solicited and selected under a minimum-development constraint may not work on an MJS spacecraft if the experiments were originally designed for the low EMI environment associated with spacecraft having shielded subsystems. This is particularly true of experiments which are susceptible to induced pulses.

Fred Scarf distributed copies of a five page letter to Ed Smith entitled "Possible Spacecraft Charging Problems Near Jupiter". It is a technical discussion of the problem and it can be made available to interested parties upon request.

The experiment teams then made four recommendations to the Project:

a) Look into the spacecraft charging problem. How serious is it likely to be? What can be done to alleviate the problem?

b) In the AFO package, state in field units the levels of EMI which an experiment package will be allowed to radiate. (Deduce these constraints from the second and third paragraphs of this report where

the acceptable levels of interference at the wave experimenters' antennas are given). Also include in the AFO package a constraint on the maximum allowable conducted interference which can be generated on experiment interface lines, namely 30 mv.

c) Consider changing the subsystem packaging and bonding philosophies so that each subsystem represents an enclosed conducting box. Consider changing the shielding philosophy so that a shield surrounding an inter-subsystem wire bundle is an extension of both subsystems' chassis - even through a connector, where the connector shell is also part of the shield envelope. Consider tight twisting and double shielding of the 50 volt AC power distribution lines within the spacecraft.

d) As soon as it becomes practical, measure the radiated and conducted interference levels associated with Viking hardware. After these results are evaluated, and prior to the issuance of a spacecraft system RFP, negotiate with the selected payload experimenters to establish the final EMI constraints that will apply to both instruments and subsystems.

APPENDIX 4

to

FINAL REPORT OF THE OPGT/MJS PLASMA WAVE SCIENCE TEAM

PLASMA WAVE TEAM ORGANIZATION AND EXPERIENCE

TEAM MEMBERS	SUCCESSFUL S/C LAUNCHES (WAVE EXPERIMENTS)	PENDING LAUNCHES
F. SCARF TRW SYSTEMS GROUP	1964-45A, OV3-3 PIONEER 8 PIONEER 9 OGO-5	IMP-H ATS-G (?)
D. GURNETT UNIVERSITY OF IOWA	INJUN 3, INJUN 5 IMP-6, S^3-A	IMP-J, HELIOS A, HELIOS B, INJUN F, ATS-G (?)
R. HELLIWELL STANFORD UNIVERSITY	OGO-1, OGO-2, OGO-3 OGO-4, OGO-6	
E. SMITH, A. FRANDSEN JET PROPULSION LAB R. HOLZER UCLA	OGO-1, OGO-2, OGO-3 OGO-4, OGO-5, OGO-6	
P. KELLOGG UNIV OF MINNESOTA	IMP-6	HELIOS A, HELIOS B
E. UNGSTRUP DANISH SPACE RESEARCH CENTER	HEOS A2	GEOS

GENERAL IMPORTANCE OF LOCAL PLASMA WAVES IN LOW DENSITY PLASMAS

- IF N IS LOW, PARTICLE-PARTICLE COLLISIONS ARE UNIMPORTANT
- WAVES ARE EASILY GENERATED IF FREE ENERGY IS AVAILABLE
- ALL ENERGY TRANSFER PROCESSES INVOLVE WAVE-PARTICLE INTERACTIONS

EXAMPLES:

1) RESISTIVE INTERACTIONS

DC ELECTRIC FIELD PRODUCES CURRENT

CURRENT PRODUCES WAVES (GENERALIZED CERENKOV EFFECT)

WAVE-PARTICLE SCATTERING TRANSFERS ENERGY INTO HEAT

(OPERATIVE AT THE BOW SHOCK, INTERPLANETARY SHOCKS, AURORAL ARCS, ETC.).

2) DIFFUSIVE INTERACTIONS

FLUCTUATING WAVE FIELDS ALLOW CHARGED PARTICLE DIFFUSION ACROSS B

PLASMA PARTICLES GAIN OR LOSE ENERGY, BECOME TRAPPED OR UNTRAPPED AS THEY MOVE INTO NEW SPATIAL REGIONS

(ACCELERATION OF VAN ALLEN BELT PARTICLES, SUBSTORM INJECTION PHENOMENA).

3) CYCLOTRON INTERACTIONS

CYCLOTRON RESONANCES PRODUCE LOCAL ACCELERATION, SCATTERING INTO LOSS-CONE, PRECIPITATION

(STABLE TRAPPING LIMIT IN THE EARTH'S MAGNETOSPHERE, MICROBURSTS, PROTON RING CURRENT DECAY).

THE ROLE OF PLASMA WAVE MEASUREMENTS FOR MJS

1. ORIGIN AND DYNAMICS OF THE JUPITER RADIATION BELTS

(SUMMARY OF RADIATION WORKSHOP MODELS)

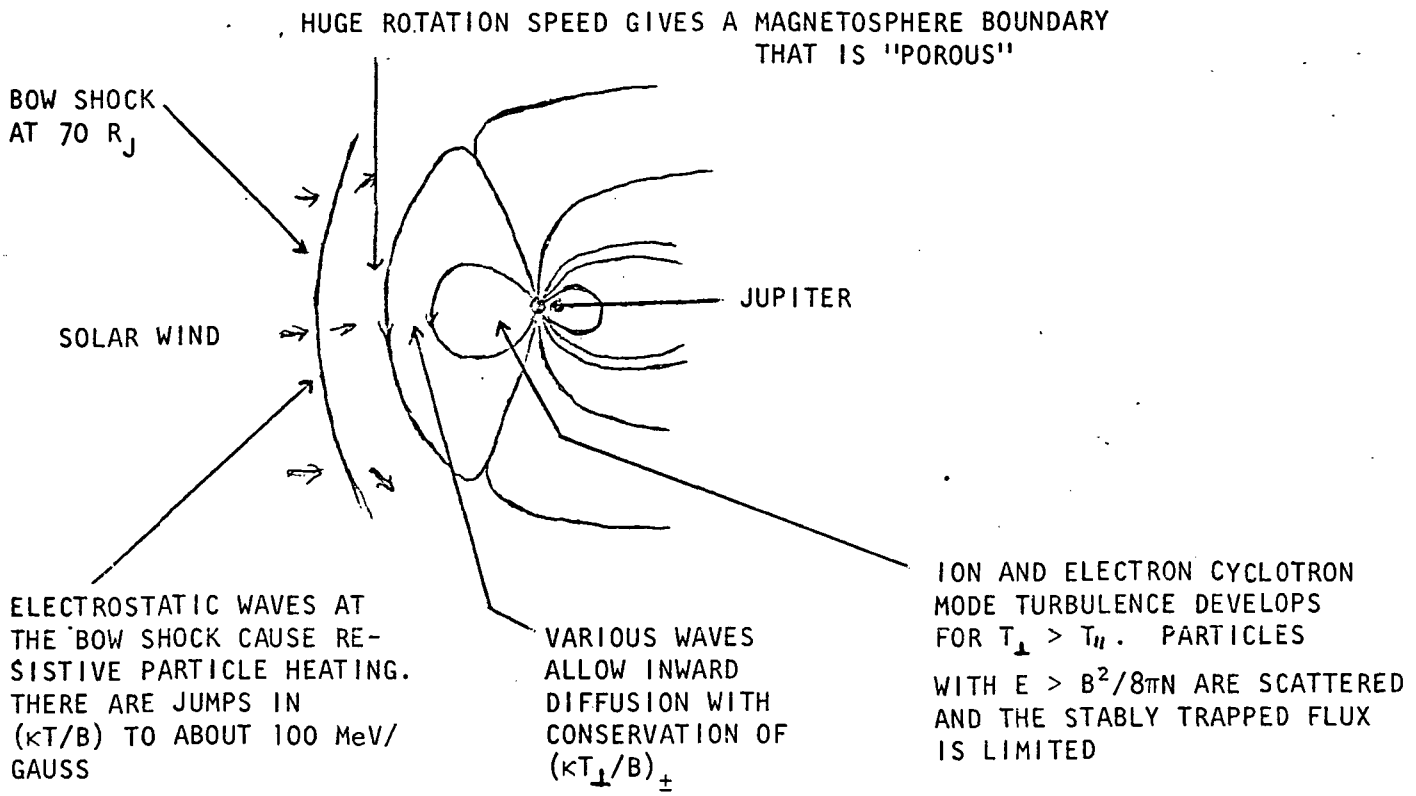

2. OTHER ASPECTS OF PARTICLE-PLASMA WAVE INTERACTIONS AT JUPITER

- CYCLOTRON RESONANT INTERACTIONS CAN LOCALLY ACCELERATE PARTICLES, IN ADDITION TO CAUSING PRECIPITATION AND DIFFUSION.
- WE KNOW THAT NEAR THE EARTH, ELECTROSTATIC WAVES ARE MOST EFFICIENT IN CAUSING SCATTERING, BUT THE RADIATION WORKSHOP MODELS IGNORE THESE MODES.
- THE IO-MODULATION OF THE DECAMETER RADIATION IS COMMONLY INTERPRETED IN TERMS OF PHENOMENA INVOLVING LOCAL PLASMA WAVES (SUCH AS TURBULENT RESISTIVITY). MILLISECOND MODULATION IS DETECTABLE AT EARTH.

THE ROLE OF MJS PLASMA WAVE MEASUREMENTS

SATURN OBJECTIVES

- THE MAGNETOSPHERE IS LIKELY TO BE SIMILAR TO THAT OF JUPITER WITH A SMALLER B (FOR $B_o \simeq 1$ GAUSS, THE ANALOG OF THE RADIATION WORKSHOP MODEL GIVES SYNCHROTRON RADIATION LEVELS UNDETECTABLE AT EARTH).
- THE INITIAL WAVE-PARTICLE HEATING AT SATURN'S BOW SHOCK MAY BE QUITE DIFFERENT BECAUSE THE 10 AU WIND IS EXPECTED TO HAVE VERY DIFFERENT PLASMA WAVE INSTABILITIES.
- THE RINGS COULD PRODUCE PLASMA WAVE EFFECTS.
- IF SATURN IS UNMAGNETIZED, IT IS SO BIG THAT THERE MUST BE A BOW SHOCK (PERHAPS AN IONOPAUSE-TYPE). EVEN IN THIS CASE, A PLASMA INSTABILITY MUST DEVELOP TO PROVIDE THE SHOCK DISSIPATION.

INTERPLANETARY AND INTERSTELLAR OBJECTIVES

- SEARCH FOR NEW FORMS OF INTERPLANETARY SHOCKS AND DISCONTINUITIES.
- OVERALL STUDY OF SOLAR WIND STABILITY, AND ITS RADIAL GRADIENT.
- SEARCH FOR THE HELIOPAUSE BOUNDARY.

THE ROLE OF PLASMA WAVE MEASUREMENTS FOR DIAGNOSTICS

1) ABSOLUTE DENSITY MEASUREMENTS IN THE SOLAR WIND

   WE DETECT $f_p^- = 9\sqrt{N}$ kHz (N IN cm^{-3}); THIS TECHNIQUE HAS BEEN EXTENSIVELY USED NEAR EARTH.

2) ABSOLUTE DENSITY MEASUREMENT IN THE MAGNETOSPHERE BY MEASUREMENT OF LHR FREQUENCY.

3) EVALUATION OF NON-LOCAL $N(\underset{\sim}{r})$, $B(\underset{\sim}{r})$ BY DETECTION AND ANALYSIS OF WHISTLERS. DETECTION OF ATMOSPHERIC LIGHTNING.

4) ABSOLUTE He^+/H^+ RATIO IN THE MAGNETOSPHERE BY MEASUREMENT OF THE CROSSOVER FREQUENCY FOR PROTON WHISTLERS.

5) USING OUR ELECTRIC FIELD SENSORS IN AN UNBALANCED MODE, WE SHOULD BE ABLE TO DETECT EFFECTS OF DIFFERENTIAL SPACECRAFT CHARGING PHENOMENA.

MJS PLASMA WAVE INSTRUMENT

MEASUREMENTS

HIGH TIME RESOLUTION BANDPASS CHANNELS

32-CHANNEL SPECTRUM ANALYZER (20 Hz-200,000 Hz)
CONTINUOUS AVERAGE READINGS
PEAK SAMPLE AND HOLD FOR IMPULSES
SWITCH FROM E TO B

WAVEFORM (ASSUMES 10 kb BUFFER)

10 TO 300 Hz E OR B WAVEFORMS
CAPTURE 1 SEC SNAPSHOTS AND READ OUT.

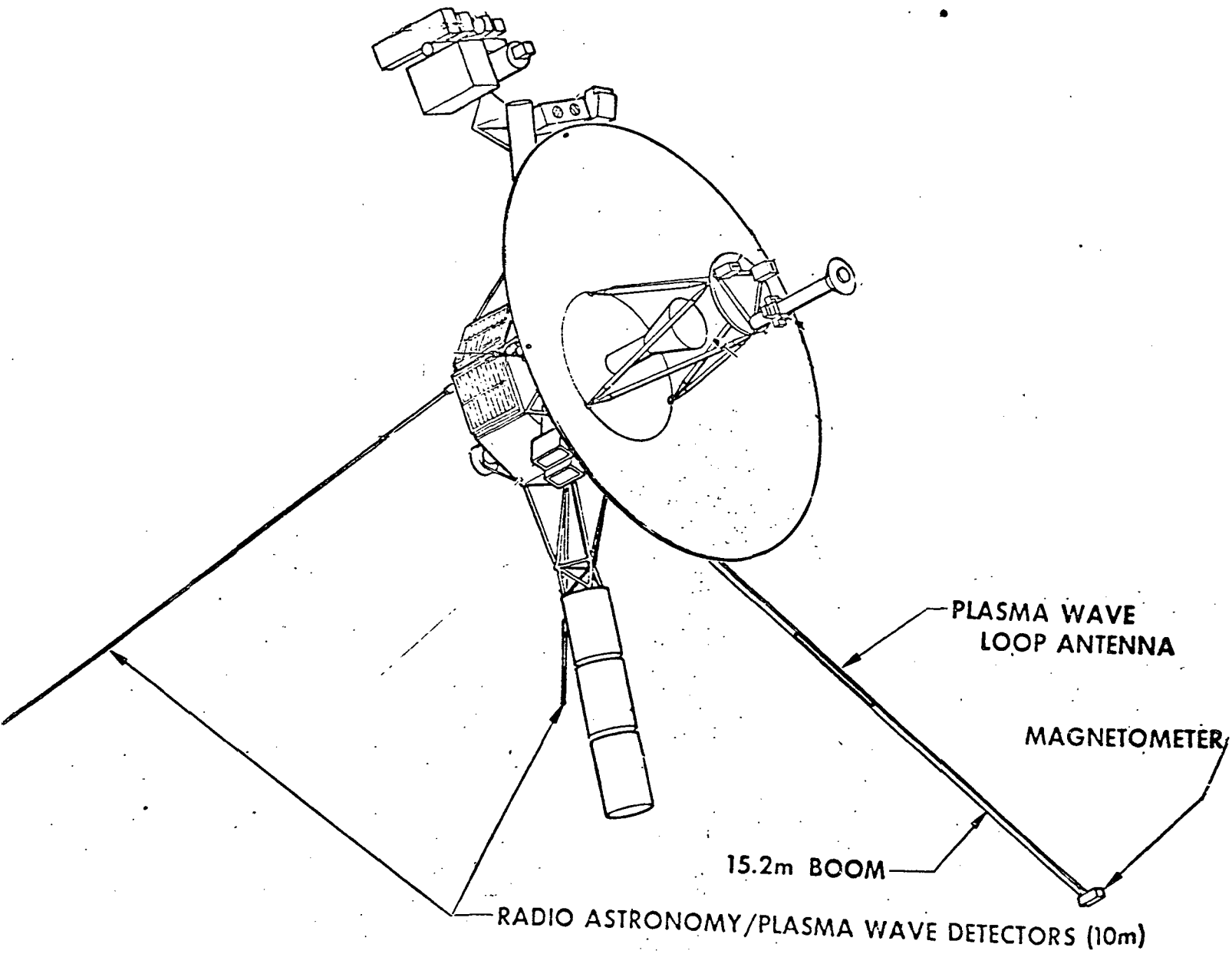

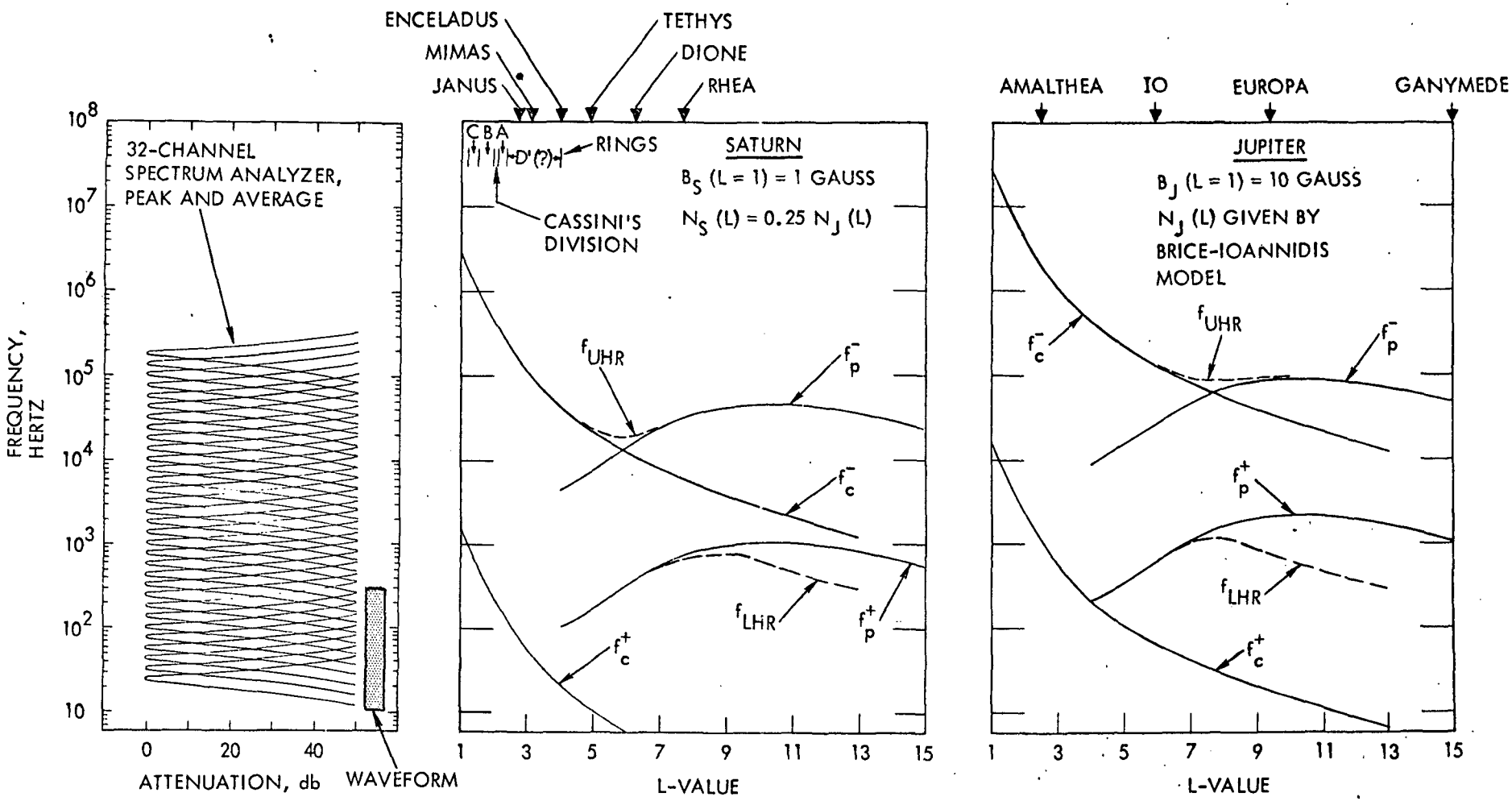
ENCELADUS
TETHYS
MIMAS
DIONE
JANUS
RHEA
AMALTHEA
IO
EUROPA
GANYMEDE
FREQUENCY, HERTZ
32-CHANNEL SPECTRUM ANALYZER, PEAK AND AVERAGE
ATTENUATION, db
WAVEFORM
C B A
D' (?)
RINGS
CASSINI'S DIVISION
SATURN
B_S (L = 1) = 1 GAUSS
N_S (L) = 0.25 N_J (L)
JUPITER
B_J (L = 1) = 10 GAUSS
N_J (L) GIVEN BY BRICE-IOANNIDIS MODEL
f_{UHR}
f_p^-
f_c^-
f_{LHR}
f_p^+
f_c^+
L-VALUE

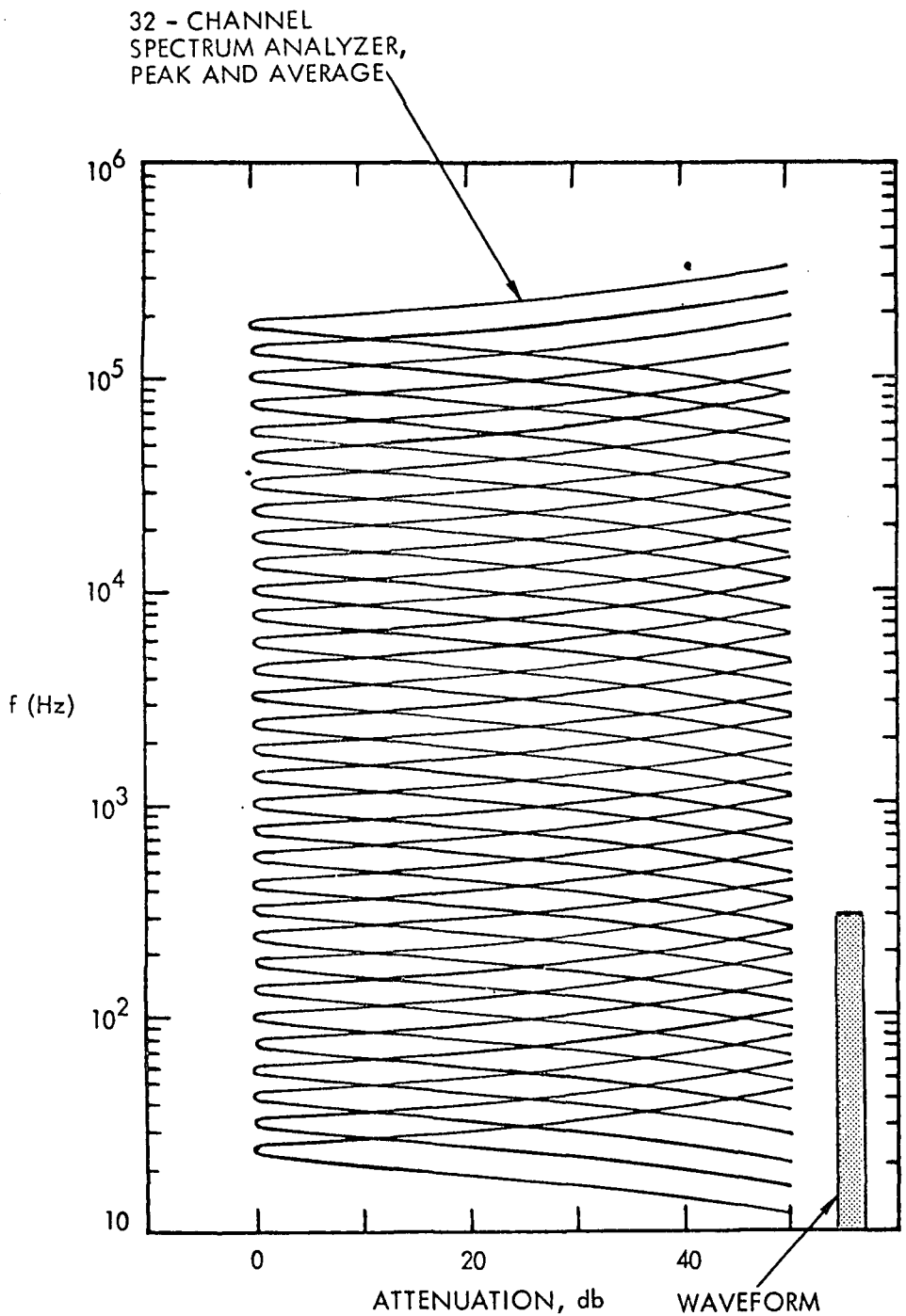
32 - CHANNEL
SPECTRUM ANALYZER,
PEAK AND AVERAGE
10^6
10^5
10^4
10^3
10^2
10
f (Hz)
0
20
40
ATTENUATION, db
WAVEFORM

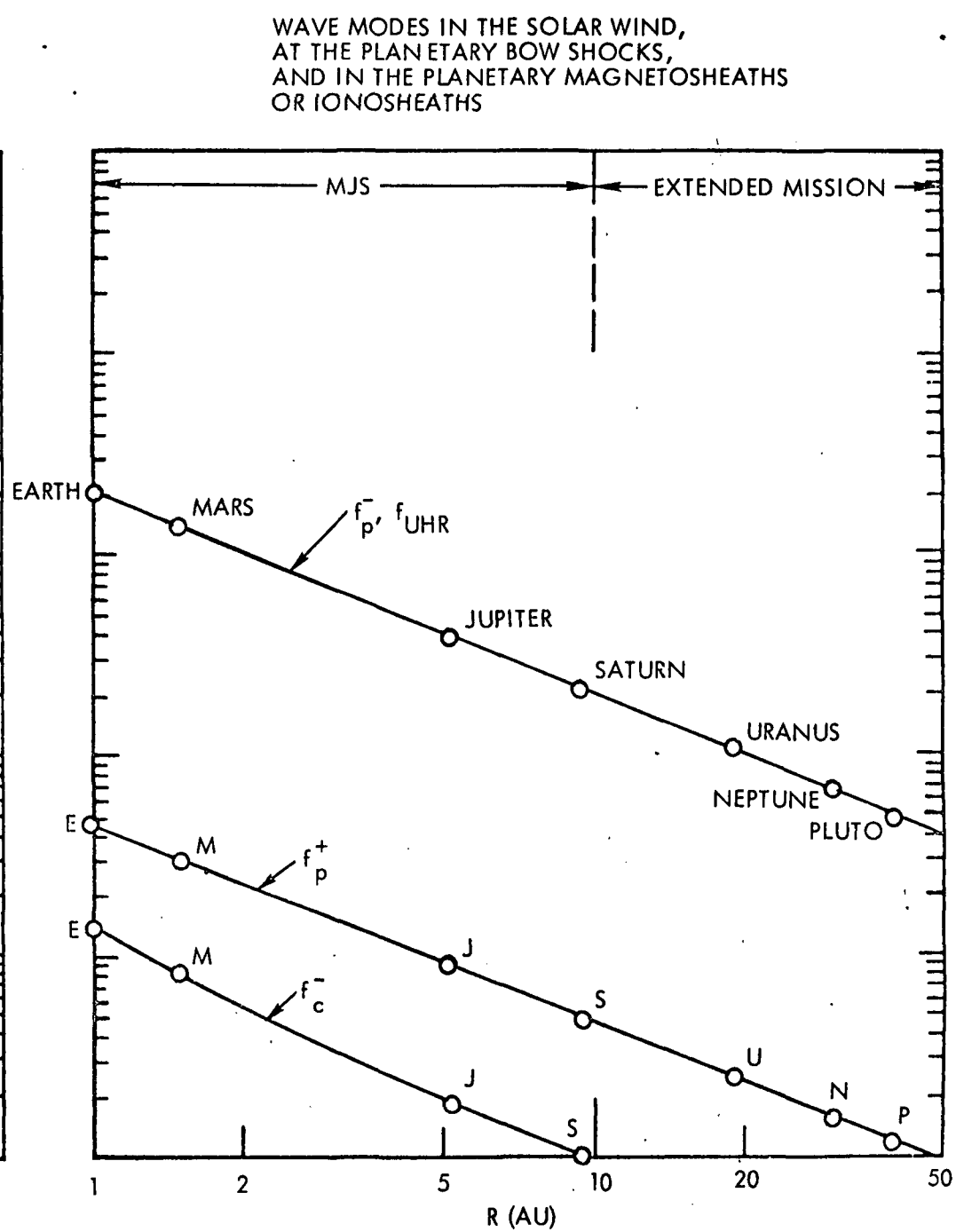
WAVE MODES IN THE SOLAR WIND,
AT THE PLANETARY BOW SHOCKS,
AND IN THE PLANETARY MAGNETOSHEATHS
OR IONOSHEATHS
MJS
EXTENDED MISSION
EARTH
MARS
f_p^-, f_{UHR}
JUPITER
SATURN
URANUS
NEPTUNE
PLUTO
E
M
f_p^+
J
S
U
N
P
E
M
f_c^-
J
S
1
2
5
10
20
50
R (AU)

MISSION REQUIREMENTS

WEIGHT: 4.0 LBS + SENSORS. POWER: 2.0 WATTS

SENSORS: WE MUST HAVE AN ELECTRIC DIPOLE; THE MAGNETIC SENSOR IS A VITAL BACKUP.

TM: WE WANT SEVERAL HUNDRED BITS/SEC AT ENCOUNTER TO OBTAIN THE NECESSARY HIGH TIME RESOLUTION.

BUFFER: WE PROPOSE TO CAPTURE AUDIO FREQUENCY (10 TO 300 Hz) WAVEFORMS THROUGHOUT THE MISSION USING A 10 kb BUFFER.

EMC CONSIDERATIONS

MARINER FACES SEVERE ELECTRICAL HAZARDS PASSING JUPITER:

- IT IS KNOWN THAT THERE WILL BE AMBIENT RF FIELDS WITH VOLT/METER AMPLITUDES.
- THERE WILL BE VLF FIELDS WITH UNDETERMINED AMPLITUDES (NO PIONEER F,G DATA).
- THERE CAN BE SEVERE SPACECRAFT CHARGING PROBLEMS (ATS-5 AND OTHER SPACECRAFT DETECT 300 V/M TO 3 keV/METER LOCAL E-FIELDS IN REGIONS OF EARTH ORBIT WHERE $\kappa T_e \sim 5$ TO 20 keV; THE JOVIAN BELTS HAVE HUNDREDS OF keV TO MeV THERMAL ENERGIES).

MEASURES MUST BE TAKEN TO PROTECT MARINER SUBSYSTEMS FROM THESE HAZARDS (ELECTRICAL SHIELDING OF THE ENTIRE SPACECRAFT, OF ALL CABLES, OF ALL SUBSYSTEMS).

THESE SAME MEASURES WILL AUTOMATICALLY SOLVE THE POTENTIAL PLASMA WAVE EMC PROBLEMS (THE ABSENCE OF SOLAR PANELS IS A GREAT HELP IN THIS AREA; THESE PANELS HAVE ALWAYS BEEN A MAJOR SOURCE OF NOISE).

18864-6004-RO-00

APPENDIX 5

to

FINAL REPORT OF THE OPGT/MJS PLASMA WAVE SCIENCE TEAM

Plasma Wave Experiment for OPGT

by

R. L. Smith and R. A. Helliwell

July 1972

Final Report

Prepared under

TRW Systems Group
Subcontract 105GB1-SC

RADIOSCIENCE LABORATORY

STANFORD ELECTRONICS LABORATORIES

STANFORD UNIVERSITY • STANFORD, CALIFORNIA

PLASMA WAVE EXPERIMENT FOR OPGT

R. L. Smith and R. A. Helliwell
Radioscience Laboratory
Stanford University
Stanford, California

Final Report

Prepared Under

TRW Systems Group
Subcontract 105GB1-SC

July 1972

CONTENTS

ILLUSTRATIONS

PLASMA WAVE EXPERIMENT FOR OPGT

R. L. Smith and R. A. Helliwell
Radioscience Laboratory
Stanford University
Stanford, California

This report deals with the proposed plasma wave experiment for the Outer Planets Grand Tour (OPGT). The emphasis is on sensitive receivers for the detection of magnetic and electric fields at very low frequencies, interference specifications, interference reduction, and interfaces with other experiments.

The results of our study reflect previous experience on five OGO spacecraft, and a previous proposal to measure electric and magnetic fields on the Jupiter mission (Pioneers F and G). Substantial parts of this report are based on work growing out of a meeting of R. L. Smith and Al Frandsen with L. H. Rorden of Develco, Inc. Mr. Rorden was the design engineer for four of the Stanford University/Stanford Research Institute vlf experiments on OGO, and also participated in the Jupiter mission proposal.

We first give a short discussion on available sensitivities of magnetic and electric sensors to form a basis for some of the later suggestions. A section on practical measured and predicted sensitivities follows. A number of specific suggestions are made for reducing interference. The problems of interfacing to related experiments are reviewed. A possible plasma wave experiment is then briefly discussed.

LOW-NOISE PREAMPLIFIERS

An excellent discussion of low noise broadband vlf receiving techniques is given by Rorden [1965]. The fundamental limitations are the noise temperature of the preamplifier, the "effective volume" of the antenna, the antenna bandwidth and the desired frequency and system bandwidth. The effective volume of a dipole is approximately

$$S_{dip} \cong \frac{\pi \ell^3}{\mathrm{Log}(\ell/a)-1}$$

where ℓ is the half length and "a" the wire radius. The effective volume of a single turn loop is

$$S_{loop} \cong \frac{\pi^2 b^3}{\mathrm{Log}(b/a)}$$

where "b" is the loop radius, and "a" the wire radius. The antenna bandwidth in radians per second is given by

$$\Omega_{dip} = G/C$$

$$\Omega_{loop} = R/L$$

for the dipole and loop, respectively, where G is the parallel conductance of a dipole with an effective capacitance C, and R is the series resistance of a loop with inductance L. These quantities are functions of the antenna geometry, size, and the amount of conducting material (mass). The effective volume, antenna bandwidth and preamplifier noise temperature set a lower limit on the minimum detectable power in a unit bandwidth at a given frequency for a narrowband system. Generally this curve has a slope of -2 with frequency (in log coordinates) as

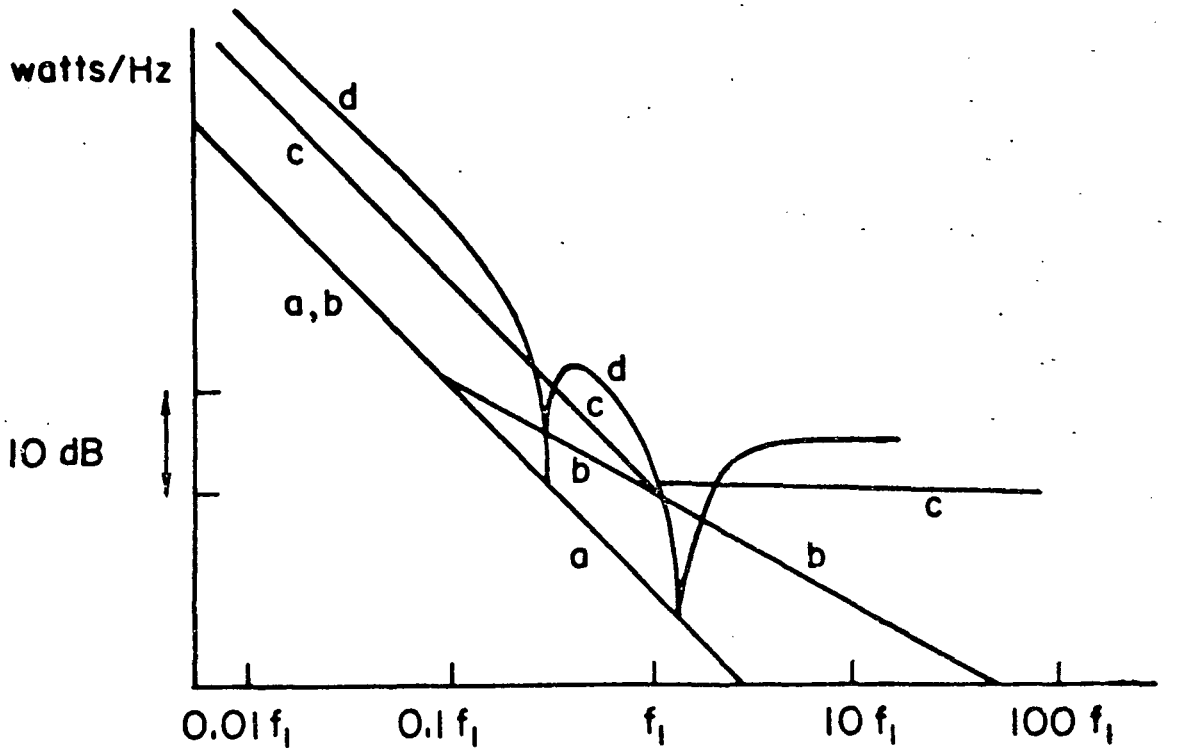

FIGURE 1. CHARACTERISTICS OF MINIMUM DETECTABLE SIGNALS. Curve "a" indicates the minimum detectable signal in a narrowband system. Curve "b" represents the locus of possible corner frequencies for a simple coupling network for a broadband system with noise characteristics of curve "c." The corner at f_1 may be moved to any position along curve "b." Curve "d" shows the result of a more complicated coupling network. No average improvement can be obtained by using complicated networks. The frequency at which curves "a" and "b" join depends on the "intrinsic bandwidth" of the antenna and the ratio of antenna temperature to noise temperature.

shown schematically by curve "a" in Figure 1.

The variation of minimum detectable signal with frequency for a broadband system depends on the nature of the coupling network between the antenna and preamplifier. For a simple coupling network, responses of the type indicated by curve "c" can be obtained, where the best obtainable noise performance can be specified at only one frequency. More complicated networks can be used to improve the noise performance in certain frequency ranges, but only at the expense of performance in other frequency ranges. This is illustrated by curve "d." Note that the frequency response gain characteristics can be obtained independently of the noise sensitivity response.

MULTI-COUPLERS

When broadband systems are contemplated for highly reactive sources (i.e., the problem at hand for either loops or dipoles for antenna sizes much less than a wavelength), one might be inclined to use a set of preamplifiers with multi-coupler elements added between the source and each amplifier. Although this problem has not received the consideration it deserves, the result of some thought and lack of any supportable counter-proposals indicates that the signal-to-noise ratio can only be degraded over that of a single amplifier by such an arrangement. The only advantages appear to be redundancy, wherein if one preamplifier fails, the other(s) might continue to work, and reduction of exposure to intermodulation distortion from strong signals widely separated in frequency. A noiseless active filter in the multi-coupler would work if one were available, but in that case the fictitious noiseless active element could just as well serve as the amplifier.

An improvement can be obtained by using separate antennas and amplifier systems, provided they are uncoupled. An alternative scheme would be to physically switch preamplifier coupling networks sequentially.

PRACTICAL SENSITIVITIES

It is reasonable to base the estimated sensitivities of interplanetary probes on prior satellites, such as EOGO's which have penetrated this space at least locally. The principles discussed above were used in the design of the Stanford University/Stanford Research Institute vlf magnetic receivers for the EOGO and POGO spacecraft. The effective volume of the OGO antennas is roughly 5 cubic meters. This may be compared with a possible OPGT antenna in the form of a rectangle 6 ft. by 6 in., using 1/4 kg of copper, which has an effective volume of 0.03 cubic meters, a loss of 22 db with respect to OGO. The frequency of optimum sensitivity for EOGO was set at 100 kHz, and that for POGO at 10 kHz. Thus the theoretical low frequency sensitivity of POGO is about 10 db better than that of EOGO. At 200 Hz the measured sensitivities were -106 db and -88 db with respect to $1\gamma/Hz^{1/2}$. If we assume that the OPGT coupling network will have a corner frequency at 3 kHz, the sensitivity will be comparable to EOGO below that frequency. At an assumed upper frequency limit of 15 kHz, the performance will be degraded from EOGO by 14 db. These various sensitivities are illustrated in Figure 2.

The laboratory measurements of the electric field sensitivities of OGO-3, assuming an effective length equal to half the length from boom tip to boom tip varies from -36 db to -53 db with respect to $1\mu V/m/Hz^{1/2}$ over the frequency range from 200 Hz to 100 kHz. This assumes that the

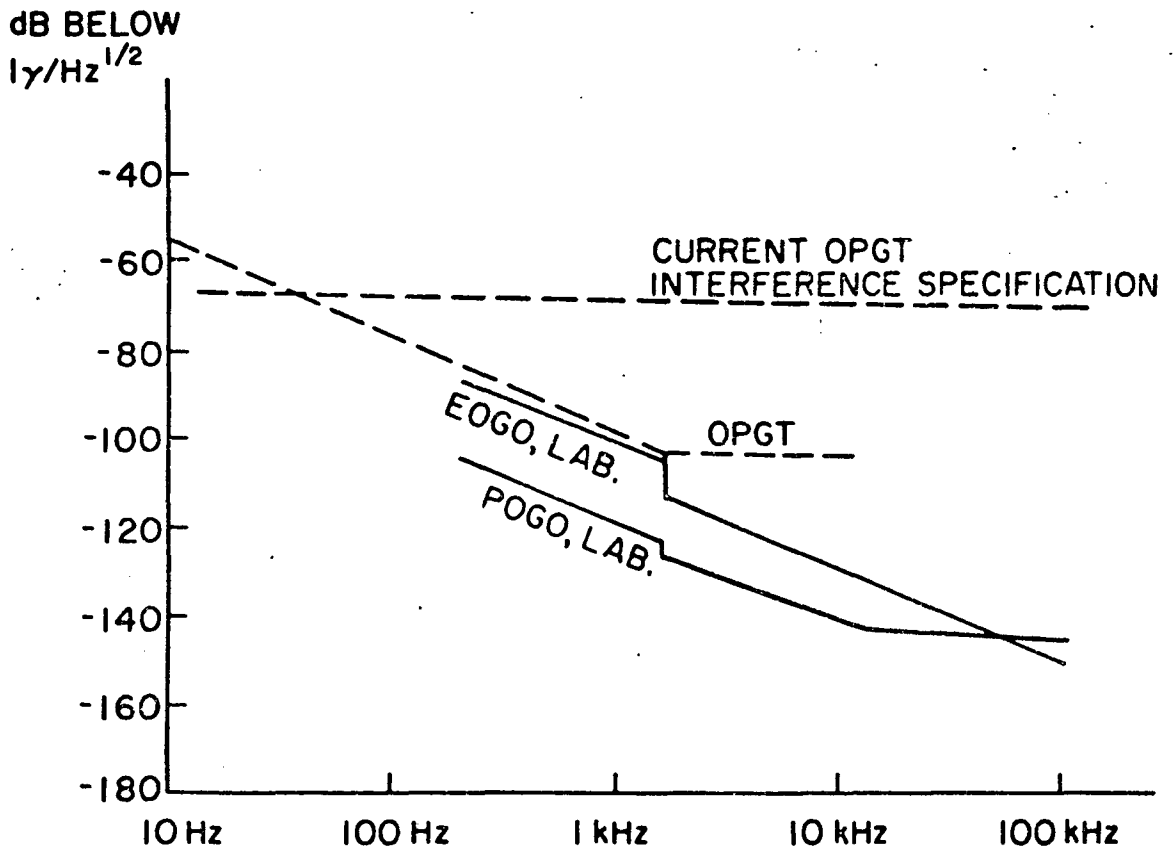

FIGURE 2. SENSITIVITIES OF EOGO, POGO, AND A POSSIBLE OPGT VLF SYSTEM OF MAGNETIC FIELD DETECTORS, COMPARED TO CURRENT OPGT INTERFERENCE SPECIFICATIONS.

antenna impedance is small compared to the input impedance. Laboratory measurements and typical in-flight noise measurements are shown in Figure 3.

SUGGESTED INTERFERENCE SPECIFICATIONS

It is somewhat difficult to translate the above figures into interference specifications of the type given in the OPGT tables because certain assumptions must be made regarding the nature of the interference. The most severe assumption is that the interference may be radiated with an intensity varying as inverse distance from, say, the main body. A somewhat relaxed assumption is an inverse square or inverse cube law. Probably the simplest approach is to assume that the sensors (antennas) will be placed one meter from the main body and use the OGO figures directly. If the sensors are placed further from the interference points, the values can be relaxed. If we assume an inverse cube variation, the equivalent interference can be increased by 18 db for each factor of 2 of the spacing of the sensors from the interference points. No OPGT specifications are indicated for electric fields in Figure 3 because the current existing specification is being rewritten.

A suggestion is made in Figures 4 and 5 for the maximum interference levels that should be permitted at the OPGT vlf experiment. In deriving these curves, the following assumptions were made: 1) The OPGT spacecraft will be no noisier than the OGO series. 2) For the magnetic levels, the same values were used below 30 Hz as given in the OPGT tables. The straight line approximation was continued for higher frequencies to a level of $10^{-15} \gamma^2/\text{Hz}$. This corresponds quite closely to the best obtainable OGO performance. 3) The levels of magnetic and

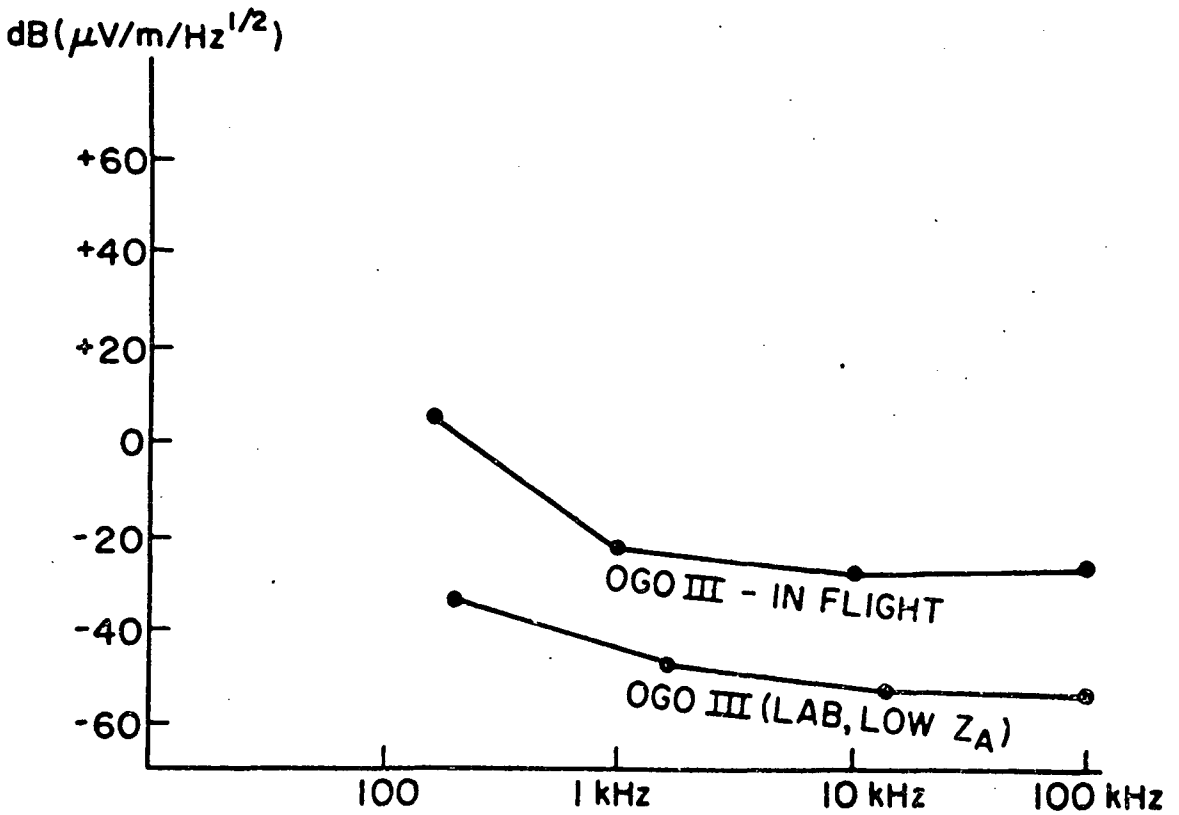

FIGURE 3. ELECTRIC FIELD SENSITIVITIES, OGO-III, BASED ON LABORATORY AND INFLIGHT MEASUREMENTS. The laboratory measurement assumed a low antenna impedance.

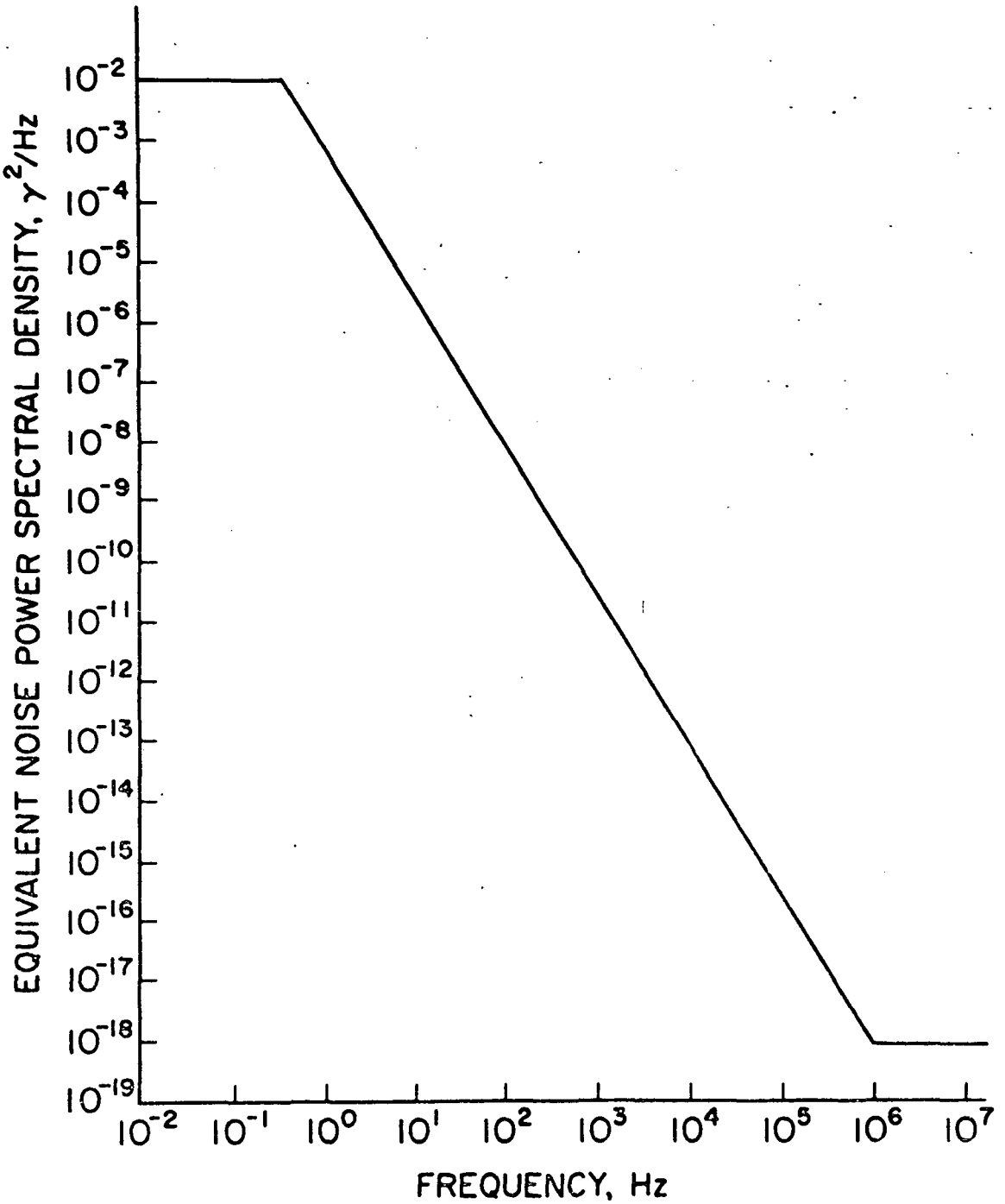

FIGURE 4. MAXIMUM ALLOWABLE DYNAMIC MAGNETIC FIELD AT ONE METER DUE TO A SUBSYSTEM.

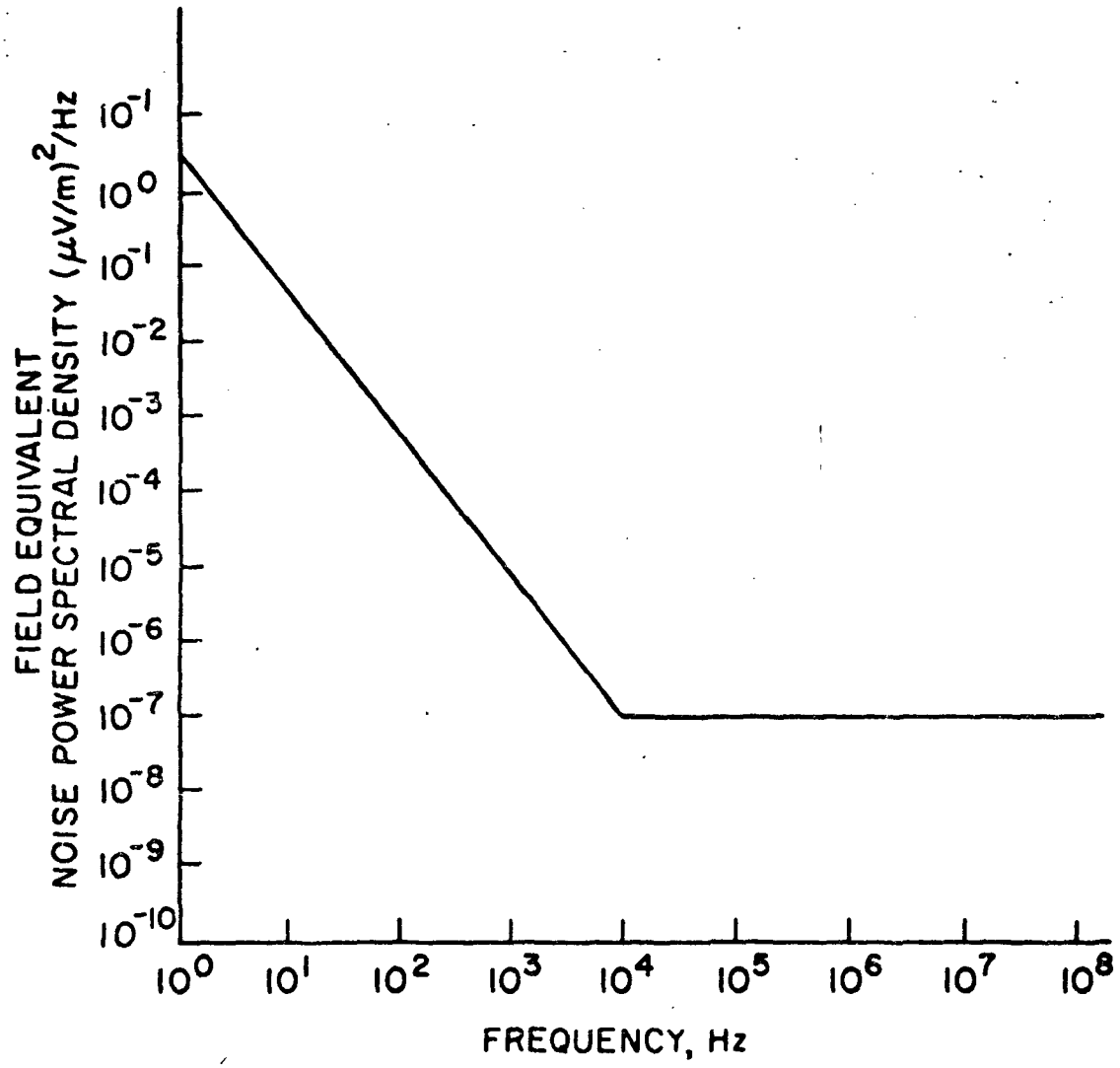

FIGURE 5. MAXIMUM ALLOWABLE GENERATED ELECTRIC FIELD INTERFERENCE LEVELS.

electric fields at 10 MHz correspond to the needs of the Radio Astronomy experiment.

SPACECRAFT SYSTEM INTERFERENCE SOURCES

Previous experience has shown that major interference sources frequently are part of the spacecraft system, especially in the power supply inverters with their associated ripple filters, and in the solar panels. Proper design and specifications can result in a low noise spacecraft. It is important to consider the noise problems before the spacecraft design becomes "frozen."

A common source of a-c magnetic interference is the ripple filter, not the inverter proper. Three specific recommendations can be made as follows:

1. Use as high an inverter frequency as possible.
2. The ripple filter toroid must be wound uniformly. This is frequently not done, with the result that very large dipole moments remain. The toroids must not be "scramble wound."
3. An eddy current shield should be made as small as possible, surrounding only the coils and transformers, not the other components. Walls of the shields should have a continuous large cross section. Fasteners, joints, etc., should be eliminated to whatever extent is feasible.

Although solar cells are not planned for OPGT, it is worth noting that there are various ways in which solar cells may cause trouble, both in planned and unplanned ways. However a great deal of trouble can be avoided if the solar cell is designed to trickle charge the battery. It is vital that all exposed potential surfaces, especially those with positive potential, be thoroughly insulated. The wires to the solar cells should be arranged to minimize loop paths. Note that voltage regulation does not of itself solve interference problems since noise currents will frequently show up as voltages on the solar array.

Each wire should be treated as a source of electric and magnetic fields. The most important wires are those which penetrate the basic spacecraft skin. Wherever possible the wires penetrating the skin should be shielded with the shield bonded to the skin as close as possible to the point of penetration.

GROUP INTERFACES

Meeting the scientific objectives through the design of an optimum set of experiments will require the cooperation of the various scientific groups. At this point the two other groups which will have the greatest influence on the Plasma Wave experiment design are the Magnetic Fields group and the Radio Astronomy group. One approach is to arrange joint meetings among members of each of the three groups (the above, plus Plasma Wave) to discuss detailed scientific problems and possible engineering compromises. Some areas of common interest are discussed below.

We are, of course, naturally concerned about possible sources of interference to the wave experiments. If, as now seems likely, the magnetic field antenna for the plasma wave experiment will be close to the magnetometer, the magnetometer becomes the most probably source of interference. The type of magnetometer chosen should produce negligible a-c fields. Flux-gate magnetometers are particularly prone to give interference.

On the other hand we must be concerned with sources of static magnetic interference to the magnetometer. We need to know in some detail the sensitivity of the magnetometer. One possible interference source is the input transformer from the magnetic loop antenna. The

size of the transformer is inversely related to the low frequency cutoff desired. If the magnetometer is sensitive to a-c magnetic fields, to a sufficiently high frequency (say, at least 100 Hz), the a-c components of the magnetometer could be coupled to the plasma wave instrument for further processing, while the low frequency cutoff of the a-c loop could be raised, thus reducing the size of the input transformer and consequent magnetic interference.

RADIO ASTRONOMY INTERFACE

The importance of the electric antenna to the plasma wave experiment is emphasized in report PW 4 in which it was concluded that "in a truly minimum plasma wave experiment, electric field measurements would take precedence over magnetic field measurements." Hopefully any differences of opinion between the Plasma Wave and Radio Astronomy Groups can be resolved so that a coordinated and readily defendable proposal can be made.

Orientation of electric antenna. According to the latest available information, TOPS configuration 3A, the electric antennas will be oriented approximately along $\pm 45^{\circ}$ lines relative to the x and y axis. Since a major objective of the Radio Astronomy group is to measure wave polarization, the symmetry of the antenna system should be examined. The most obvious source of asymmetry is the 50 ft. magnetometer boom in the -y direction. The parasitic nature of the boom will cause coupling between the two antennas. It is not clear that the presence of this boom has been taken into account as a parasitic element. It could have a considerable effect on polarization measurements.

The most sensitive arrangement is to operate a monopole antenna in

the +y direction opposite the long boom. In this way the remainder of the spacecraft becomes in essence the other part of an unbalanced dipole, with an effective length half the distance from end to end. The other antenna system would be in the ±x direction. This orientation would probably interfere with the numerous optical experiments presently placed opposite the boom. This possibility could nevertheless be examined for other possible spacecraft.

Feed point of electric antennas. The overall signal-to-inteference ratio of an electric antenna depends on the location of the feed point. The principal source of interference is presumably other experiments and spacecraft functions. Except for radiation from large objects, like solar panels, the source size may be considered small compared with antenna dimensions (assuming a large antenna appropriate to radio astronomy). In a balanced configuration the signal strength will fall roughly linearly as the feed point is moved outward, but the interference signal strength should be reduced at a higher inverse power of feed point distance. This implies that an optimum feed point exists which is neither at the antenna tip nor at the satellite base connection. The optimum point of feeding may not be known but can perhaps be estimated using assumed interference sources. Since we propose to share electric antennas with the Radio Astronomy group, the input interface becomes vital. As discussed previously, the maximum sensitivity is obtained by having a single preamplifier for each sensor. A multi-coupler may be used after the preamplifier to give the appropriate frequency band to each experiment. When a single sensor is used over a wide frequency range, the signal-to-noise ratio will be degraded in some frequency bands (see the section on low noise preamplifiers).

The frequency band from 15 kHz to 100 kHz is important because of high-pass noise, band-limited noise, and type III solar noise bursts. According to the present plan, this frequency range will be covered by the radio astronomy portion of the experiment. If there is any possibility that this band will not be covered by the Radio Astronomy group, we must be informed in sufficient time to be able to propose that it be covered by the Plasma Wave group.

DUAL SWEEPING EXPERIMENT

One interesting possibility for an experiment utilizing multiple antennas, say two dipoles and a loop, is to use two sweeping receivers with switchable preamplifiers. The following options are then available:

1. Measure electric and magnetic fields simultaneously.
2. Measure electric field polarization.
3. Measure the dispersive characteristics of electric field signals using offset sweeping of the receivers.
4. Measure the dispersive characteristics of magnetic field signals.
5. Provide redundancy in case one system fails.

Such a system can be built using two bands for each receiver, covering say 20 to 800 Hz with a 12 Hz bandwidth and 800 to 14,000 Hz with a 200 Hz bandwidth. The main body package of EOGO, designed 10 years ago, weighed only 800 gms (1.75 lbs.) and used less than 1 watt of power. It is, therefore, likely that such a system described above could be built within the weight and power limitations of the OPGT. Such a system would require adding only a preamplifier to the circuitry suggested by Frandsen and Martin [1971].

LOGARITHMIC SWEEPING RECEIVER

In the normal mode of operation of sweeping receivers an equal

amount of time is spent on each frequency interval, or else certain frequencies are skipped. As a general principle, it would appear more useful to be able to frequency-scan in logarithmic increments with logarithmic bandwidths. The first approximation to this principle is to use multiple sweeping receivers, as in the OGO series, for example.

There is another possibility that may be used in low data rate systems. Suppose the rate of frequency stepping is controlled in a quantized nearly logarithmic fashion by suitable feedback around the digital frequency control circuits. The highest stepping rate occurs at some multiple of the data rate, but all frequencies are covered. The amplitude of the detected outputs is summed, even though a range of frequencies may be covered, and the output is read out, then reset, at each major data cycle. The effect is then quite similar to the use of multiple filters with logarithmic bandwidths and frequency separations. If more frequency resolution is required, the receiver can be readily commanded, or internally controlled, to resume a linear sweep.

REFERENCES

Frandsen, A. M. A. and D. P. Martin, Preliminary minimum experiment description (instrument portion only) for the combined OPGT Plasma Wave and Planetary Radio Astronomy Experiments, November 19, 1971.

Rorden, L. H., A study of low-noise broadband vlf receiving techniques, Tech. Rept., Stanford Research Institute, Menlo Park, Calif., November 1965.